

 Open access • Journal Article • DOI:10.1103/PHYSREVB.95.165440

## Partition-free theory of time-dependent current correlations in nanojunctions in response to an arbitrary time-dependent bias — [Source link](#)

Michael Ridley, Angus MacKinnon, Lev Kantorovich

**Institutions:** Imperial College London, King's College London

**Published on:** 24 Apr 2017 - Physical Review B (American Physical Society)

**Topics:** Quantum noise, Spectral density and Hamiltonian (quantum mechanics)

Related papers:

- [Time-dependent partition-free approach in resonant tunneling systems](#)
- [Current through a multilead nanojunction in response to an arbitrary time-dependent bias](#)
- [Time-dependent transport in interacting and noninteracting resonant-tunneling systems](#)
- [Time-dependent Landauer-Buttiker formula: application to transient dynamics in graphene nanoribbons](#)
- [Time-dependent quantum transport: Direct analysis in the time domain](#)

Share this paper:    

View more about this paper here: <https://typeset.io/papers/partition-free-theory-of-time-dependent-current-correlations-4j6qbcj374>

# Partition-free theory of time-dependent current correlations in nanojunctions in response to an arbitrary time-dependent bias

Michael Ridley,<sup>1</sup> Angus MacKinnon,<sup>1</sup> and Lev Kantorovich<sup>2</sup>

<sup>1</sup>*Department of Physics, The Blackett Laboratory, Imperial College London, South Kensington Campus, London SW7 2AZ, United Kingdom*

<sup>2</sup>*Department of Physics, King's College London, Strand, London, WC2R 2LS, United Kingdom*

(Received 10 November 2016; revised manuscript received 28 February 2017; published 24 April 2017)

Working within the nonequilibrium Green's function formalism, a formula for the two-time current correlation function is derived for the case of transport through a nanojunction in response to an arbitrary time-dependent bias. The one-particle Hamiltonian and the wide-band limit approximation are assumed, enabling us to extract all necessary Green's functions and self-energies for the system, extending the analytic work presented previously [Ridley *et al.*, *Phys. Rev. B* **91**, 125433 (2015)]. We show that our expression for the two-time correlation function generalizes the Büttiker theory of shot and thermal noise on the current through a nanojunction to the time-dependent bias case including the transient regime following the switch-on. Transient terms in the correlation function arise from an initial state that does not assume (as is usually done) that the system is initially uncoupled, i.e., our approach is partition free. We show that when the bias loses its time dependence, the long-time limit of the current correlation function depends on the time difference only, as in this case an ideal steady state is reached. This enables derivation of known results for the single-frequency power spectrum and for the zero-frequency limit of this power spectrum. In addition, we present a technique which facilitates fast calculations of the transient quantum noise, valid for arbitrary temperature, time, and voltage scales. We apply this formalism to a molecular wire system for both dc and ac biases, and find a signature of the traversal time for electrons crossing the wire in the time-dependent cross-lead current correlations.

DOI: [10.1103/PhysRevB.95.165440](https://doi.org/10.1103/PhysRevB.95.165440)

## I. INTRODUCTION

Electronic devices with nanoscale dimensions can now be fabricated and tuned to form active circuit components [1]. In addition to the speedup in processing power that arises from submicrometer size [2], molecular junctions also enable a massive speedup in device operation due to THz intramolecular transport processes and fast electron traversal time [3]. Subsequent to the initial proposal of molecular rectification in 1974 [4], chemical fabrication techniques have led to the realization of many interesting devices, including molecular wires [5,6], single-electron transistors [7], frequency doublers and detectors [8,9], and switches for fast memory storage [10,11]. In addition, conductance properties of nanostructures subjected to strong time-dependent external fields have been the subject of intense experimental research. This research includes work on photon-assisted tunneling (PAT) [12,13] and transport through ac-biased carbon-based nanostructures in the GHz-THz regime [14–17].

In contrast to classical electronics, the time-dependent current in molecular structures may undergo fluctuations that have a comparable magnitude to the current signal itself, so that a theory of time-dependent fluctuations is essential for the design and control of these devices [18]. Moreover, time-dependent current-current correlations and their associated frequency-dependent noise spectra contain information which is not present in the first moment of the current [19]. This includes deviation from classical behavior in the Fano factor due to Pauli repulsion [20,21], detection of fractional charges for quantum Hall quasiparticles [22], and the determination of transmission probabilities [23]. When the external field driving the transport process depends upon time, the transient current correlations provide information on intramolecular “circular” currents that cannot be studied using the current alone [24].

Recent measurements of shot noise in graphene irradiated by THz fields showed an enhancement of the shot noise due to the excitation of electron-hole pairs in the sample [25].

In general, nanoelectronic devices possess noise spectra which are nonlinear functions of frequency. When in equilibrium, there are two regimes, namely, the low- $\omega$  regime, in which Johnson-Nyquist noise is evident [26,27], and the high- $\omega$  scenario, in which zero-point fluctuations dominate [28]. When a bias is applied to the system, one observes in addition the shot noise, which results from the discreteness of electronic charge and the Pauli exclusion principle. At high frequencies, it was shown that the correct noise spectra are an asymmetric function of the frequency due to the dominance of zero-point photon fluctuations there [28,29]. Distinct negative and positive frequency components of the current noise due to quasiparticle tunneling across a Josephson junction have been measured experimentally [30], and may be physically interpreted in terms of the transfer of energy quanta during the corresponding absorption and emission processes [31]. In the theoretical literature, both symmetric [32–35] and asymmetric [36–38] noise spectra have been classified and studied.

The Landauer-Büttiker (LB) theory of shot and thermal noise represents a significant milestone in the development of the theory of current fluctuations in nanoscale systems [19,33,34,39,40]. Originally, it was developed within a scattering matrix approach to coherent quantum transport, wherein one typically considers a molecular junction as a subsystem coupled to macroscopic leads, which act as heat and particle reservoirs. Electrons in the leads are treated as independent plane waves, populated according to the Fermi distribution function, and propagated onto the molecule, where they scatter. Experiments have demonstrated a good agreement between experiment and the noise spectra obtained from the

scattering theory for both the low-frequency noise [41,42] and for power spectra that depend upon the frequency of the measurement device [28,43,44]. In these studies the scattering potential is chosen to be static, but time-dependent scattering formalisms have been developed which enable the calculation of current and current noise in response to an ac potential in the leads [45–47], in both the adiabatic [45] and nonadiabatic [48,49] regimes. These approaches make use of the Floquet theorem, as do master-equation approaches, which expand scattering states into a harmonic series [35,50], generating functional approaches to the full counting statistics (FCS) [51] and reduced density matrix methods that make a perturbative expansion in the lead-molecule coupling [52]. The noise response to an ac field has been shown to carry information on the production of electron-hole pairs that does not appear in the noise response to a dc bias [53]. Moreover, these electron-hole pairs are correlated and able to propagate through the molecular junction into separate terminals [54,55]. In a generating functional approach to the full counting statistics of an ac-driven system, it was proven that a periodic Lorentzian voltage signal with quantized flux minimized the noise, i.e., it was reduced to the dc level [56,57]. In recent experiments, these quantized voltage pulses, known as *levitons*, have been experimentally realized [58] and approximated by a biharmonic driving field [59]. Even given the restriction of periodic time dependence, one can study a rich range of phenomena, such as photon-assisted tunneling (PAT) [35,54,60,61], quantum pumping [62,63], and the interplay of external driving field parameters with Fabry-Pérot conductance oscillations in graphene nanoribbon (GNR) and carbon nanotube (CNT) systems [64].

The nonequilibrium Green's function (NEGF) or Keldysh method for the calculation of dynamical quantum statistical averages can be used to reexpress time-dependent transmission functions, currents, and particle populations in terms of products of self-energies and Green's functions [65–68]. The equivalence of this picture to the Landauer-Büttiker theory in the noninteracting case is well known [69,70]. However, it can also be extended to perturbative calculations of noise in systems with a Coulombic interaction [63,71] and to the derivation of steady-state fluctuation-dissipation relations involving the current-current correlation functions of quantum dots coupled to a single-phonon mode [72]. Crucially for this work, it involves the propagation of Green's functions along a complex time contour that means the effects of the equilibrium preparation of the system are automatically taken into account in the dynamics resulting from the switch-on of a bias in the leads [68].

Many calculations of the time-dependent response of a nanojunction to the switch-on of a bias across the junction make use of the *partitioned* approach, in which the leads and molecule are completely decoupled prior to the switch on time  $t_0$ , and suddenly coupled simultaneously with the addition of a time-dependent bias to the leads at  $t_0$  [73–76]. Partitioned approaches often involve relegation of  $t_0$  to the distant past because in noninteracting systems the memory-loss theorem [77] guarantees that the initial condition does not affect the long-time dynamics. However, transient dynamics was also studied within a partitioned approach following an artificial

quench that instantaneously couples the molecule to the leads, as was recently done for phononic transport [78] (assuming that such an experiment can be done in practice). In the *partition-free* framework, one includes a coupling between the leads and molecule in the equilibrium Hamiltonian which describes the preparation of the system prior to the switch-on. Partition-free approaches to quantum transport have been implemented within NEGF [77,79] and master-equation [80] approaches. Recent calculations of transient noise characteristics have made use of the partitioned approach [63,81,82], and there are currently no published calculations of the transient current noise arising from a partition-free switch-on process.

In recent years, partition-free generalizations of the LB formula for the current and particle number response to the switch-on of a static bias have been derived [68,83–85]. This formalism makes use of the wide-band limit approximation (WBLA), and enables fast calculation of the transport characteristics of realistic systems at very low computational cost compared with other time-dependent schemes [85–87]. It was then extended by the present authors to the current response to an arbitrary time-dependent bias [88], and a practical scheme for implementation of this formula based upon the replacement of all frequency integrals with special functions was then developed [89,90]. In the static bias partition-free switch-on approach pioneered in Refs. [68,84,85], an analytic result for the *equal time* lesser Green's function  $\mathbf{G}^<(t,t)$  was derived, from which the particle number in the molecular region and current in the leads can be derived. However, to calculate current-current correlations one needs an expression for the lesser Green's function in the two-time plane  $\mathbf{G}^<(t_1,t_2)$ , and the formalism presented in Refs. [88,89,91] does this for the arbitrarily time-dependent bias. The ability to deal with arbitrary time dependence enables us to study a wider class of switch-on problems, including those in which the bias is stochastic in time [91]. In this work, we will extend our NEGF method further in order to develop an exact formalism enabling the study of transient current correlations resulting from an *arbitrary* time-dependent bias in the leads. This method does not involve any assumption of adiabaticity or weak lead-molecule coupling, and neither is there any limitation on the kind of time dependence which can be studied. This will be useful within the field of fast noise calculations for real molecular junctions driven by ultrafast pulses [3,24,92], and to new physics arising from the time-resolved nanoelectronic response to these pulses that includes the effects of the initial coupling.

The paper is organized as follows. In Sec. II, we introduce the partition-free time-dependent NEGF formalism developed in Refs. [88,89,91], and show how to obtain generic formulas for the two-time current correlation function within the WBLA. In Sec. III, expressions are derived for the long-time and static bias approximations in the frequency domain, thereby confirming that our formalism agrees with other published work. In Sec. IV, we present the results of numerical calculations of the two-time current correlations in a two-terminal nanojunction, based upon a fast algorithm that is based on an expansion of the Fermi function with subsequent analytic removal of all frequency integrals. We calculate the time-dependent cross correlations for extended

molecular wires of different sizes. We identify finite-size effects in the transient current cross correlations which cannot be observed in single-level systems. In particular, by studying the competition between wire length, end-site coupling, and internal coupling on the molecule, we show that a resonant signature of the time taken for electronic information to cross the system can be seen in both the transient and steady-state cross-lead correlations.

## II. PARTITION-FREE CORRELATION FUNCTION

### A. Time-dependent NEGF

In quantum transport processes, one is typically concerned with the time-dependent electronic response through a junction at measurement time  $t$  to the switch-on of a bias at some initial time  $t_0$ , which drives the system away from equilibrium. The equations of motion for quantum statistical averages are evolved along a complex time contour, consisting of an upper branch  $C_-$  running from  $t_0 + i0$  to  $t + i0$ , then along a lower branch  $C_+$  running back from  $t - i0$  to  $t_0 - i0$ , and finally along the imaginary-time branch  $C_M$  from  $t_0 - i0$  to  $t_0 - i\beta$ , where  $\beta \equiv 1/k_B T$  (it is adopted that  $\hbar = 1$  in the following). The structure of this contour is suggested by the mathematical structure of the quantum statistical ensemble average associated with the operator  $\hat{O}(t)$ :

$$O(t) = Z^{-1} \text{Tr}[e^{-\beta \hat{H}^M} U^\dagger(t, t_0) \hat{O}(t) U(t, t_0)]. \quad (1)$$

In this expression,  $\hat{H}^M$  denotes the Matsubara Hamiltonian describing the equilibrium system,  $Z = \text{Tr}[e^{-\beta \hat{H}^M}]$  is the partition function of the system, and the  $U$  ( $U^\dagger$ ) are propagators describing the evolution of the nonequilibrium system after the bias is switched on. Thus, real times taken on the horizontal branches of the Konstantinov-Perel' contour correspond to the nonequilibrium system, whereas on the vertical branch of the contour the equilibrium system is represented. More detail on the meaning of the contour can be found in Ref. [68].

The Hamiltonian we will use to describe the junction is formally identical to the one studied in Ref. [91] and is parametrized by the variable  $z$  which denotes the contour "time" variable specifying positions on the Konstantinov-Perel' contour  $\gamma \equiv C_- \oplus C_+ \oplus C_M$ :

$$\begin{aligned} \hat{H}(t) = & \sum_{k\alpha} \varepsilon_{k\alpha}(z) \hat{a}_{k\alpha}^\dagger \hat{a}_{k\alpha} + \sum_{mn} H_{mn}(z) \hat{d}_m^\dagger \hat{d}_n \\ & + \sum_{m,k\alpha} [T_{mk\alpha}(z) \hat{d}_m^\dagger \hat{a}_{k\alpha} + T_{k\alpha m}(z) \hat{a}_{k\alpha}^\dagger \hat{d}_m]. \end{aligned} \quad (2)$$

Here,  $\hat{a}_{k\alpha}$ ,  $\hat{d}_m$  and  $\hat{a}_{k\alpha}^\dagger$ ,  $\hat{d}_m^\dagger$  are annihilation and creation operators of leads and central system electronic states, where for simplicity spin degrees of freedom are neglected. The first term is a Hamiltonian of the lead states  $k$  belonging to each lead  $\alpha$ , the second is the Hamiltonian of the molecule sandwiched between the leads, describing hopping within the molecular structure, and the third term describes the coupling of the molecule to the leads. We collect elements of this Hamiltonian into a matrix consisting of "blocks" corresponding to each of the physical subsystems it describes. For example, the  $\alpha - C$

"block" is the matrix  $\mathbf{h}_{\alpha C}(z)$  with elements  $V_{k\alpha, m}(z)$ :

$$\mathbf{h}(z) = \begin{pmatrix} \mathbf{h}_{11}(z) & 0 & \cdots & \mathbf{h}_{1C}(z) \\ 0 & \mathbf{h}_{22}(z) & \cdots & \mathbf{h}_{2C}(z) \\ \vdots & \vdots & \ddots & \vdots \\ \mathbf{h}_{C1}(z) & \mathbf{h}_{C2}(z) & \cdots & \mathbf{h}_{CC}(z) \end{pmatrix}. \quad (3)$$

In the molecular basis, we also define the  $(i, j)$ th component of the one-particle Green's function on the Konstantinov-Perel' contour:

$$G_{ij}(z_1, z_2) = -i \frac{\text{Tr}\{e^{-\beta \hat{H}^M} \hat{T}_\gamma [\hat{d}_{i,H}(z_1) \hat{d}_{j,H}^\dagger(z_2)]\}}{\text{Tr}[e^{-\beta \hat{H}^M}]}. \quad (4)$$

The elements  $G_{ij}$  of the Green's function form a matrix  $\mathbf{G}$  defined on the whole space of orbitals of all leads and the central region; correspondingly, one can introduce diagonal,  $\mathbf{G}_{CC}$  and  $\mathbf{G}_{\alpha\alpha}$ , as well as nondiagonal,  $\mathbf{G}_{C\alpha}$ ,  $\mathbf{G}_{\alpha C}$ , and  $\mathbf{G}_{\alpha\alpha'}$ , blocks of this matrix:

$$\mathbf{G}(z_1, z_2) = \begin{pmatrix} \mathbf{G}_{11}(z_1, z_2) & \mathbf{G}_{12}(z_1, z_2) & \cdots & \mathbf{G}_{1C}(z_1, z_2) \\ \mathbf{G}_{21}(z_1, z_2) & \mathbf{G}_{22}(z_1, z_2) & \cdots & \mathbf{G}_{2C}(z_1, z_2) \\ \vdots & \vdots & \ddots & \vdots \\ \mathbf{G}_{C1}(z_1, z_2) & \mathbf{G}_{C2}(z_1, z_2) & \cdots & \mathbf{G}_{CC}(z_1, z_2) \end{pmatrix}. \quad (5)$$

The Green's function  $\mathbf{G}_{CC}$  for the central region is obtained by projecting the general equation of motion onto the  $CC$  matrix block:

$$\begin{aligned} \left[ i \frac{d}{dz_1} - \mathbf{h}_{CC}(z_1) \right] \mathbf{G}_{CC}(z_1, z_2) \\ = \mathbf{1}_{CC} \delta(z_1, z_2) + \int_\gamma d\bar{z} \boldsymbol{\Sigma}_{CC}(z_1, \bar{z}) \mathbf{G}_{CC}(\bar{z}, z_2), \end{aligned} \quad (6)$$

where  $\mathbf{1}_{CC}$  is the unit matrix in the  $C$  subspace, and

$$\boldsymbol{\Sigma}_{CC}(z_1, z_2) = \sum_\alpha \mathbf{h}_{C\alpha}(z_1) \mathbf{g}_{\alpha\alpha}(z_1, z_2) \mathbf{h}_{\alpha C}(z_2) \quad (7)$$

is the matrix of the embedding self-energy, where  $\mathbf{g}_{\alpha\alpha}(z_1, z_2)$  is the isolated lead Green's function, whose evolution is governed solely by the  $\alpha\alpha$  block of the Hamiltonian matrix (3). The nondiagonal matrix blocks of the Green's function are given by Eqs. (A1) and (A2) in Appendix A. The blocks in Eq. (5) can then be further subdivided into subspaces defined by regions of the complex time plane. For example, the "left" Green's function  $\mathbf{G}^\leftarrow$  is obtained by choosing  $z_1 \in C_M$  and  $z_2 \in C_\mp$ , and one can obtain its equation of motion using the Langreth rules [93,94]:

$$\begin{aligned} \mathbf{G}_{CC}^\leftarrow(\tau_1, t_2) \left[ -i \overleftarrow{\frac{d}{dt_2}} - \mathbf{h}_{CC}(t_2) \right] \\ = [\mathbf{G}_{CC}^\leftarrow \cdot \boldsymbol{\Sigma}_{CC}^a + \mathbf{G}_{CC}^M \star \boldsymbol{\Sigma}_{CC}^\leftarrow]_{(\tau_1, t_2)}, \end{aligned} \quad (8)$$

where the differential operator in the left-hand side acts on the left. In this expression, the convolution integrals denoted by " $\cdot$ " and " $\star$ " are defined in Eqs. (A3) and (A4), respectively. One also defines the "right" Green's function  $\mathbf{G}^\rightarrow$  by choosing

$z_1 \in C_{\mp}$  and  $z_2 \in C_M$ , the “lesser” and “greater” Green’s functions  $\mathbf{G}^{\lessgtr}$  with, e.g.,  $z_1 \in C_-$ ,  $z_2 \in C_+$  and  $z_1 \in C_+$ ,  $z_2 \in C_-$ , respectively, and the Matsubara Green’s function  $\mathbf{G}^M$  with  $z_1, z_2 \in C_M$ . In addition, “retarded” and “advanced” Green’s functions are stipulated with a definite real-time ordering:

$$\mathbf{G}^r(t_1, t_2) = \theta(t_1, t_2)[\mathbf{G}^>(t_1, t_2) - \mathbf{G}^<(t_1, t_2)], \quad (9)$$

$$\mathbf{G}^a(t_1, t_2) = -\theta(t_2, t_1)[\mathbf{G}^>(t_1, t_2) - \mathbf{G}^<(t_1, t_2)]. \quad (10)$$

The equations obtained by projecting Eq. (6) and its complex conjugate onto these subregions of the complex time plane are known as the Kadanoff-Baym equations (see, e.g., Ref. [68]).

### B. Generalized expression from Wick’s theorem

The current in lead  $\alpha$  can be obtained as the thermal average of the time derivative of the average charge in that lead  $I_{\alpha}(t) \equiv q \langle \frac{d\hat{N}_{\alpha}(t)}{dt} \rangle$  (where the spin-degenerate particle number is  $\hat{N}_{\alpha} = 2 \sum_k \hat{d}_{k\alpha}^{\dagger} \hat{d}_{k\alpha}$ ). In all numerical calculations that follow, the electron charge will be set to  $q = -1$ . Given the noninteracting Hamiltonian in Eq. (2), the current operator has the form

$$\hat{I}_{\alpha}(t) = 2iq \sum_{k,m} [T_{mk\alpha}(t) \hat{d}_m^{\dagger}(t) \hat{d}_{k\alpha}(t) - T_{mk\alpha}^*(t) \hat{d}_{k\alpha}^{\dagger}(t) \hat{d}_m(t)]. \quad (11)$$

We define the current deviation operator with a mean value of zero:

$$\Delta \hat{I}_{\alpha}(t) = 2iq \sum_{k,m} [T_{mk\alpha}(t) (\hat{d}_m^{\dagger}(t) \hat{d}_{k\alpha}(t) - \langle \hat{d}_m^{\dagger}(t) \hat{d}_{k\alpha}(t) \rangle) - T_{mk\alpha}^*(t) (\hat{d}_{k\alpha}^{\dagger}(t) \hat{d}_m(t) - \langle \hat{d}_{k\alpha}^{\dagger}(t) \hat{d}_m(t) \rangle)]. \quad (12)$$

The two-time current correlator between leads  $\alpha$  and  $\beta$  is defined as

$$C_{\alpha\beta}(t_1, t_2) \equiv \langle \Delta \hat{I}_{\alpha}(t_1) \Delta \hat{I}_{\beta}(t_2) \rangle. \quad (13)$$

This correlator obviously satisfies the symmetry property

$$C_{\alpha\beta}(t_1, t_2)^* = C_{\beta\alpha}(t_2, t_1). \quad (14)$$

Since  $\Delta \hat{I}_{\alpha}(t_1)$  and  $\Delta \hat{I}_{\beta}(t_2)$  do not commute in general,  $C_{\alpha\beta}(t_1, t_2)$  is not guaranteed to be real and so in several studies the symmetrized correlation function is preferred [33,34]:

$$P_{\alpha\beta}(t_1, t_2) \equiv \frac{1}{2} \langle \Delta \hat{I}_{\alpha}(t_1) \Delta \hat{I}_{\beta}(t_2) + \Delta \hat{I}_{\beta}(t_2) \Delta \hat{I}_{\alpha}(t_1) \rangle = \text{Re}[C_{\alpha\beta}(t_1, t_2)]. \quad (15)$$

Since  $P_{\alpha\beta}(t_1, t_2)$  is just the real part of  $C_{\alpha\beta}(t_1, t_2)$ , knowledge of the latter object is sufficient for a full characterization of the symmetric noise properties of the junction. The lack of two-particle interactions in the Hamiltonian (2) means we can simplify the nonsymmetrized correlator using Wick’s theorem, which is valid for a noninteracting Hamiltonian with arbitrary time dependence [68]:

$$C_{\alpha\beta}(t_1, t_2) = -4q^2 \sum_{k,k',m,m'} [T_{mk\alpha}(t_1) T_{m'k'\beta}(t_2) \langle \hat{d}_m^{\dagger}(t_1) \hat{d}_{k'\beta}(t_2) \rangle \langle \hat{d}_{k\alpha}(t_1) \hat{d}_{m'}^{\dagger}(t_2) \rangle - T_{mk\alpha}(t_1) T_{m'k'\beta}^*(t_2) \langle \hat{d}_m^{\dagger}(t_1) \hat{d}_{m'}(t_2) \rangle \langle \hat{d}_{k\alpha}(t_1) \hat{d}_{k'\beta}^{\dagger}(t_2) \rangle - T_{mk\alpha}^*(t_1) T_{m'k'\beta}(t_2) \langle \hat{d}_{k\alpha}^{\dagger}(t_1) \hat{d}_{k'\beta}(t_2) \rangle \langle \hat{d}_m(t_1) \hat{d}_{m'}^{\dagger}(t_2) \rangle + T_{mk\alpha}^*(t_1) T_{m'k'\beta}^*(t_2) \langle \hat{d}_{k\alpha}^{\dagger}(t_1) \hat{d}_{m'}(t_2) \rangle \langle \hat{d}_m(t_1) \hat{d}_{k'\beta}^{\dagger}(t_2) \rangle]. \quad (16)$$

One identifies the following Green’s functions in this expression:

$$[\mathbf{G}_{AB}^>(t_1, t_2)]_{kk'} = -i \langle \hat{d}_{kA}(t_1) \hat{d}_{k'B}^{\dagger}(t_2) \rangle, \quad (17)$$

$$[\mathbf{G}_{AB}^<(t_1, t_2)]_{kk'} = i \langle \hat{d}_{k'B}^{\dagger}(t_2) \hat{d}_{kA}(t_1) \rangle, \quad (18)$$

where  $A$  and  $B$  correspond to either the lead or central molecule regions. It is then possible to rewrite Eq. (15) in the compact analytic form

$$C_{\alpha\beta}(t_1, t_2) = -4q^2 \text{Tr}_C [\mathbf{h}_{C\alpha}(t_1) \mathbf{G}_{\alpha C}^>(t_1, t_2) \mathbf{h}_{C\beta}(t_2) \mathbf{G}_{\beta C}^<(t_2, t_1) - \mathbf{h}_{\alpha C}(t_1) \mathbf{G}_{\alpha\beta}^>(t_1, t_2) \mathbf{h}_{\beta C}(t_2) \mathbf{G}_{CC}^<(t_2, t_1) - \mathbf{G}_{CC}^>(t_1, t_2) \mathbf{h}_{C\beta}(t_2) \mathbf{G}_{\beta\alpha}^<(t_2, t_1) \mathbf{h}_{\alpha C}(t_1) + \mathbf{G}_{C\beta}^>(t_1, t_2) \mathbf{h}_{\beta C}(t_2) \mathbf{G}_{C\alpha}^<(t_2, t_1) \mathbf{h}_{\alpha C}(t_1)]. \quad (19)$$

The expression (19) is structurally identical to current correlation functions in Refs. [24,82], but we emphasize that here the two-time Green’s functions appearing in Eq. (19) evolve in response to the switch-on of an arbitrary time-dependent bias in the partition-free approach, i.e., they contain convolution integrals taken along the vertical part of the Konstantinov-Perel’ contour as well. Notice that, in addition to correlation functions describing particle hopping events between the leads and the molecule, Eq. (19) also contains information on lead-lead hopping events and on “circular” [24] currents involving electronic transport processes within the molecular structure. In some work on the time-dependent noise, the two-time correlator was given as a function of a single time [81], but we emphasize that we need to solve the Kadanoff-Baym equations for all Green’s functions “blocks” in Eq. (5) in the two-time plane for a complete picture of current fluctuations. We present the main steps of this derivation in Appendix A, and the derived Green’s functions are inserted into Eq. (19), resulting in a sum of terms involving only self-energy components and components of the  $CC$  region Green’s function:

$$C_{\alpha\beta}(t_1, t_2) = 4q^2 \text{Tr}_C [(\Sigma_{\alpha}^>(t_1, t_2) \delta_{\alpha\beta} + [(\Sigma_{\alpha}^> \cdot \mathbf{G}_{CC}^> + \Sigma_{\alpha}^r \cdot \mathbf{G}_{CC}^> + \Sigma_{\alpha}^{\neg} \star \mathbf{G}_{CC}^r) \cdot \Sigma_{\beta}^a + \Sigma_{\alpha}^r \cdot (\mathbf{G}_{CC}^r \cdot \Sigma_{\beta}^> + \mathbf{G}_{CC}^{\neg} \star \Sigma_{\beta}^r)]_{(t_1^{\dagger}, t_2^{\dagger})}) \mathbf{G}_{CC}^<(t_2, t_1) + \mathbf{G}_{CC}^>(t_1, t_2) (\Sigma_{\alpha}^<(t_2, t_1) \delta_{\alpha\beta} + [(\Sigma_{\beta}^< \cdot \mathbf{G}_{CC}^a + \Sigma_{\beta}^r \cdot \mathbf{G}_{CC}^< + \Sigma_{\beta}^{\neg} \star \mathbf{G}_{CC}^r) \cdot \Sigma_{\alpha}^a + \Sigma_{\beta}^r \cdot (\mathbf{G}_{CC}^r \cdot \Sigma_{\alpha}^< + \mathbf{G}_{CC}^{\neg} \star \Sigma_{\alpha}^r)]_{(t_2^{\dagger}, t_1^{\dagger})})]$$



$$\begin{aligned}
& - (\boldsymbol{\Sigma}_\alpha^> \cdot \mathbf{G}_{CC}^a + \boldsymbol{\Sigma}_\alpha^r \cdot \mathbf{G}_{CC}^> + \boldsymbol{\Sigma}_\alpha^\top \star \mathbf{G}_{CC}^\top)_{(t_1^+, t_2^-)} (\boldsymbol{\Sigma}_\beta^< \cdot \mathbf{G}_{CC}^a + \boldsymbol{\Sigma}_\beta^r \cdot \mathbf{G}_{CC}^< + \boldsymbol{\Sigma}_\beta^\top \star \mathbf{G}_{CC}^\top)_{(t_2^-, t_1^+)} \\
& - (\mathbf{G}_{CC}^> \cdot \boldsymbol{\Sigma}_\beta^a + \mathbf{G}_{CC}^r \cdot \boldsymbol{\Sigma}_\beta^> + \mathbf{G}_{CC}^\top \star \boldsymbol{\Sigma}_\beta^\top)_{(t_1^+, t_2^-)} (\mathbf{G}_{CC}^< \cdot \boldsymbol{\Sigma}_\alpha^a + \mathbf{G}_{CC}^r \cdot \boldsymbol{\Sigma}_\alpha^< + \mathbf{G}_{CC}^\top \star \boldsymbol{\Sigma}_\alpha^\top)_{(t_2^-, t_1^+)}. \quad (20)
\end{aligned}$$

Here, the sign superscripts indicate the contour position of each time variable. So far, no assumptions have been made on the system Hamiltonian, i.e., we have not yet stated which regions are subject to a time-dependent perturbation, and neither have we made assumptions about the nature of the lead-molecule coupling. Up to this point, the derivation is completely algebraic, and so for noninteracting systems Eq. (20) is completely general.

### C. Time-dependent model and the WBLA

In this section we make assumptions on the model that enable us to solve the Kadanoff-Baym equations analytically. We assume that, prior to  $t_0$ , the Hamiltonian  $\hat{H}_0 \equiv \hat{H}(z \in C_M)$  is given by Eq. (2) with time-independent energies  $\varepsilon_{k\alpha}(z \in C_M) = \varepsilon_{k\alpha}$  and molecular site and hopping integrals  $H_{mn}(z \in C_M) = h_{mn}$ . The lead-molecule couplings  $T_{m,k\alpha}(z \in \gamma) = T_{m,k\alpha}$  are assumed to be present in equilibrium in the partition-free approach and unchanged by the switch-on process. As all subsystems are coupled during their equilibration, they all possess the same initial temperature  $T$  and chemical potential  $\mu$ , which means the system is initially described by the density operator  $\hat{\rho}_0 = Z^{-1} e^{-\beta(\hat{H}_0 - \mu\hat{N})}$  (where  $Z$  is the partition function and  $\hat{N}$  is the number operator for the entire coupled system). Following Ref. [91], we add an arbitrary spatially homogeneous time-dependent shift to the lead energies as their bias. To the molecular Hamiltonian, we add a static correction  $\mathbf{u}_{CC} = \sum_{mn} u_{mn} \hat{d}_m^\dagger \hat{d}_n$  [85], and a

time-dependent shift that scales the particle number operator  $\hat{N}_C = \sum_{mn} \hat{d}_m^\dagger \hat{d}_n$  [91]:

$$\varepsilon_{k\alpha}(z \in C_\mp) = \varepsilon_{k\alpha} + V_\alpha(t), \quad (21)$$

$$H_{mn}(z \in C_\mp) = h_{mn} + u_{mn} + \delta_{mn} V_C(t). \quad (22)$$

Now, we assume that the leads satisfy the WBLA, i.e., we neglect the energy dependence of the lead-molecule coupling. As described in Ref. [88], this assumption enables us to write all components of the effective embedding self-energy in terms of the level-width matrix  $\Gamma_\alpha$ , defined as

$$\Gamma_{\alpha,mn} = 2\pi \sum_k T_{m,k\alpha} T_{k\alpha,n} \delta(\varepsilon_\alpha^F - \varepsilon_{k\alpha}), \quad (23)$$

where  $\varepsilon_\alpha^F$  is the equilibrium Fermi energy of lead  $\alpha$ . The self-energy components for this problem are collected together in Eqs. (B5)–(B10) of Appendix B, where the time dependence of the lead states is contained in phase factors of the form

$$\psi_\alpha(t_1, t_2) \equiv \int_{t_2}^{t_1} d\tau V_\alpha(\tau). \quad (24)$$

Within the WBLA, the KB equations [66] for the different components of  $\mathbf{G}_{CC}$  are linearized in terms of the effective Hamiltonian  $\tilde{\mathbf{h}}_{CC}^{\text{eff}} \equiv \tilde{\mathbf{h}}_{CC} - \frac{i}{2} \sum_\alpha \Gamma_\alpha$  of the central region, where  $\tilde{\mathbf{h}}_{CC} = \mathbf{h}_{CC} + \mathbf{u}_{CC}$ . The derivation of these components was published in Refs. [88,91], and leads to the following compact formula for the greater and lesser Green's functions:

$$\mathbf{G}_{CC}^{\gtrless}(t_1, t_2) = \mp i \int \frac{d\omega}{2\pi} f[\mp(\omega - \mu)] \sum_\gamma \mathbf{S}_\gamma(t_1, t_0; \omega) \Gamma_\gamma \mathbf{S}_\gamma^\dagger(t_2, t_0; \omega), \quad (25)$$

where we introduce the matrix

$$\mathbf{S}_\alpha(t, t_0; \omega) \equiv e^{-i\tilde{\mathbf{h}}_{CC}^{\text{eff}}(t-t_0)} e^{-i\varphi_C(t, t_0)} \left[ \mathbf{G}_{CC}^r(\omega) - i \int_{t_0}^t d\bar{t} e^{-i(\omega\mathbf{I} - \tilde{\mathbf{h}}_{CC}^{\text{eff}})(\bar{t}-t_0)} e^{i(\varphi_C - \psi_\alpha)(\bar{t}, t_0)} \right] \quad (26)$$

defined in terms of  $\mathbf{G}_{CC}^r(\omega) = (\omega\mathbf{I} - \mathbf{h}_{CC}^{\text{eff}})^{-1}$  (i.e., defined without the tilde on the effective Hamiltonian), and the phase factor associated with the molecular time dependence:

$$\varphi_C(t_1, t_2) \equiv \int_{t_2}^{t_1} d\tau V_C(\tau). \quad (27)$$

All other components of the Green's function (GF) can be explicitly calculated in the time domain [88,91], and are listed in Appendix B. The quantum statistical expectation value of the current operator (11) can also be reformulated as a sum of convolution integrals on the Konstantinov-Perel' contour, which may be evaluated exactly within the WBLA. Setting the electronic charge  $q = -1$ , the current may be expressed in terms of the  $\mathbf{S}_\alpha$  as [89]

$$I_\alpha(t) = \frac{1}{\pi} \int d\omega f(\omega - \mu) \text{Tr}_C \left[ 2 \text{Re}[i\Gamma_\alpha e^{i\omega(t-t_0)} e^{i\psi_\alpha(t, t_0)} \mathbf{S}_\alpha(t, t_0; \omega)] - \Gamma_\alpha \sum_\gamma \mathbf{S}_\gamma(t, t_0; \omega) \Gamma_\gamma \mathbf{S}_\gamma^\dagger(t, t_0; \omega) \right]. \quad (28)$$

The WBLA enables us to derive a closed form for the current correlation function. We substitute Eqs. (B5) and (B6) for the retarded/advanced self-energies into Eq. (20), which then reduces to a rather compact form

$$C_{\alpha\beta}(t_1, t_2) = 4q^2 \text{Tr}_C(\delta_{\alpha\beta}(\Sigma_\alpha^>(t_1, t_2)\mathbf{G}_{CC}^<(t_2, t_1) + \mathbf{G}_{CC}^>(t_1, t_2)\Sigma_\alpha^<(t_2, t_1)) + \Gamma_\alpha \mathbf{G}_{CC}^>(t_1, t_2)\Gamma_\beta \mathbf{G}_{CC}^<(t_2, t_1) + i\mathbf{G}_{CC}^>(t_1, t_2)[\Lambda_\beta^+(t_2, t_1)\Gamma_\alpha + \Gamma_\beta(\Lambda_\alpha^+)^{\dagger}(t_1, t_2)] + i[\Lambda_\alpha^-(t_1, t_2)\Gamma_\beta + \Gamma_\alpha(\Lambda_\beta^-)^{\dagger}(t_2, t_1)]\mathbf{G}_{CC}^<(t_2, t_1) - \Lambda_\beta^+(t_2, t_1)\Lambda_\alpha^-(t_1, t_2) - (\Lambda_\alpha^+)^{\dagger}(t_1, t_2)(\Lambda_\beta^-)^{\dagger}(t_2, t_1)). \quad (29)$$

Here, we have collected convolution integrals on the Konstantinov-Perel' contour into the objects  $\Lambda_\alpha^\pm(t_1, t_2)$ :

$$\Lambda_\beta^+(t_2, t_1) \equiv (\Sigma_\beta^< \cdot \mathbf{G}_{CC}^a + \Sigma_\beta^\top \star \mathbf{G}_{CC}^\top)_{(t_2^-, t_1^+)}, \quad (30)$$

$$(\Lambda_\alpha^+)^{\dagger}(t_1, t_2) \equiv -(\mathbf{G}_{CC}^r \cdot \Sigma_\alpha^< + \mathbf{G}_{CC}^\top \star \Sigma_\alpha^\top)_{(t_2^-, t_1^+)}, \quad (31)$$

$$\Lambda_\alpha^-(t_1, t_2) \equiv (\Sigma_\alpha^> \cdot \mathbf{G}_{CC}^a + \Sigma_\alpha^\top \star \mathbf{G}_{CC}^\top)_{(t_1^+, t_2^-)}, \quad (32)$$

$$(\Lambda_\beta^-)^{\dagger}(t_2, t_1) \equiv -(\mathbf{G}_{CC}^r \cdot \Sigma_\beta^> + \mathbf{G}_{CC}^\top \star \Sigma_\beta^\top)_{(t_1^+, t_2^-)}. \quad (33)$$

We may now perform the convolution integrals in Eqs. (30)–(33) using the formulas obtained for the self-energies and GFs of the  $CC$  region in Appendix B. The convolution integrals in  $\Lambda^\pm$  are evaluated using the methods of Refs. [88,91], where the transformation from Matsubara summations to frequency integrals [68] is done taking account of the ordering of time variables on the contour. This guarantees the linearity of each term in the fermion/hole distribution function  $f[\pm(\omega - \mu)]$ , and results in the following pair of functional identities:

$$\Lambda_\beta^+(t_2, t_1) = ie^{-i\psi_\beta(t_2, t_0)} \int \frac{d\omega}{2\pi} f(\omega - \mu) e^{-i\omega(t_2 - t_0)} \Gamma_\beta \mathbf{S}_\beta^\dagger(t_1, t_0; \omega), \quad (34)$$

$$\Lambda_\alpha^-(t_1, t_2) = -ie^{-i\psi_\alpha(t_1, t_0)} \int \frac{d\omega}{2\pi} [1 - f(\omega - \mu)] e^{-i\omega(t_1 - t_0)} \Gamma_\alpha \mathbf{S}_\alpha^\dagger(t_2, t_0; \omega). \quad (35)$$

Here, we have expressed  $\Lambda_\alpha^\pm$  in terms of the matrix  $\mathbf{S}_\alpha$  defined in Eq. (26). Notice on the second line of Eq. (29) the presence of the object  $4q^2 \text{Tr}_C[\Gamma_\alpha \mathbf{G}_{CC}^>(t_1, t_2)\Gamma_\beta \mathbf{G}_{CC}^<(t_2, t_1)]$ . In the single-level case, all the objects inside the trace are replaced by scalars, and this object is equal to  $q^2 \Gamma_\alpha \Gamma_\beta N_C(t)[1 - N_C(t)]$ , where the particle number on the molecular region is defined by  $N_C(t) = -2i \text{Tr}_C[\mathbf{G}_{CC}^<(t, t)]$ . The time dependence of this object is thus entirely due to the internal dynamics of electron and hole populations on sites of the molecule. The lead-dependent matrices  $\Lambda_\beta^+$  and  $\Lambda_\alpha^-$  correspond physically to electrons propagating from lead  $\beta$  and positively charged holes propagating from lead  $\alpha$ , respectively. We therefore interpret the two terms appearing on the second line of Eq. (29) as describing processes in which electrons in the leads interfere with holes in the molecular region, or holes in the leads interfere with electrons in the molecule. The terms on the third line of Eq. (29) are interpreted as cross-lead particle-hole interference terms.

In Refs. [88,91], the greater and lesser Green's functions were expressed in terms of the  $\mathbf{S}_\alpha$  matrices following a line integral of the Kadanof-Baym equations in the two-time plane, and these are given in Eq. (25). We thus have explicit formulas for all terms which appear in the two-time correlation function, which may be evaluated numerically in the  $(t_1, t_2)$  plane as follows:

$$C_{\alpha\beta}(t_1, t_2) = 4q^2 \int \frac{d\omega}{2\pi} \frac{d\omega'}{2\pi} [1 - f(\omega - \mu)] f(\omega' - \mu) \text{Tr}_C \left\{ \delta_{\alpha\beta} \sum_\gamma (\Gamma_\alpha e^{-i\psi_\alpha(t_1, t_2)} e^{-i\omega(t_1 - t_2)} \mathbf{S}_\gamma(t_2, t_0; \omega') \Gamma_\gamma \mathbf{S}_\gamma^\dagger(t_1, t_0; \omega) + \text{H.c.}) \right. \\ + \sum_{\gamma, \gamma'} \Gamma_\alpha \mathbf{S}_\gamma(t_1, t_0; \omega) \Gamma_\gamma \mathbf{S}_\gamma^\dagger(t_2, t_0; \omega) \Gamma_\beta \mathbf{S}_{\gamma'}(t_2, t_0; \omega') \Gamma_{\gamma'} \mathbf{S}_{\gamma'}^\dagger(t_1, t_0; \omega') \\ + i \sum_\gamma [\Gamma_\alpha \mathbf{S}_\gamma(t_1, t_0; \omega) \Gamma_\gamma \mathbf{S}_\gamma^\dagger(t_2, t_0; \omega) \Gamma_\beta (e^{-i\psi_\beta(t_2, t_0)} e^{-i\omega'(t_2 - t_0)} \mathbf{S}_\beta^\dagger(t_1, t_0; \omega') - e^{i\psi_\alpha(t_1, t_0)} e^{i\omega'(t_1 - t_0)} \mathbf{S}_\alpha(t_2, t_0; \omega'))] \\ - (e^{-i\psi_\beta(t_2, t_0)} e^{-i\omega(t_2 - t_0)} \Gamma_\beta \mathbf{S}_\beta^\dagger(t_1, t_0; \omega) e^{-i\psi_\alpha(t_1, t_0)} e^{-i\omega'(t_1 - t_0)} \Gamma_\alpha \mathbf{S}_\alpha^\dagger(t_2, t_0; \omega') \\ \left. + e^{i\psi_\alpha(t_1, t_0)} e^{i\omega(t_1 - t_0)} \mathbf{S}_\alpha(t_2, t_0; \omega) \Gamma_\alpha e^{i\psi_\beta(t_2, t_0)} e^{i\omega'(t_2 - t_0)} \mathbf{S}_\beta(t_1, t_0; \omega') \Gamma_\beta) \right\}. \quad (36)$$

This expression contains a great deal of information, and it is the central result of this paper. It is the two-time correlation function for a molecular junction connected to an arbitrary

number of leads, through which time-dependent voltages are passed. It contains transient parts which decay as  $t_1, t_2 \rightarrow \infty$ , while  $\tau \equiv t_1 - t_2$  remains finite. It automatically enables

evaluation of cross-correlation functions between different leads when  $\alpha \neq \beta$ , and the correlation between currents through the same lead when  $\alpha = \beta$ . It describes the noise on the current signal due to nonzero temperatures (the thermal noise), and due to a nonzero bias (the shot noise), as will be made clearer in the next section. The leads are assumed to satisfy the WBLA, and the additive contribution of the voltage to the lead-state energies is assumed, but the approach is otherwise exact for noninteracting electrons. Under close inspection, using the definition (26), we find that the explicit time dependence enters into (36) only within structures of the form  $e^{i(\psi_\alpha - \varphi_C)(t, t_0)}$ , so that the noise does not distinguish between external fields that bias all leads identically [ $V_\alpha(t) = V(t)$ , for all  $\alpha$ ] or a gate voltage which moves energies in the negative energy direction [ $V_C(t) = -V(t)$ ]. This is also true for the current [91]. The expression (36) will be used for the proof of analytic identities in Sec. III, but it is not entirely convenient for numerical evaluation. Instead, we describe in Sec. IV and Appendix D how to evaluate Eq. (29) directly.

### III. RECOVERY OF KNOWN RESULTS FOR A STATIC BIAS

To parametrize our system with experimentally relevant variables, we work in the relative time coordinate system so that  $t_1 = \tau + t$  and  $t_2 = t$ , where  $\tau \equiv t_1 - t_2$  is the relative time that we wish to take a Fourier transform with respect to  $\tau$ . Note that, to make the mapping to the Fourier space associated with  $\tau$ , one needs  $\tau$  to take on negative values. However, since both  $t_1$  and  $t_2$  must be times greater than  $t_0$ , this means that  $\tau$  is restricted to lie in the range  $[-(t - t_0), t - t_0]$ , as was done in Ref. [71]. We define the Fourier transform of the correlation with respect to the *relative time*  $\tau \equiv t_1 - t_2$ , as a function of a single frequency  $\Omega$  and the *measurement time*  $t$ :

$$\begin{aligned} P_{\alpha\beta}(\Omega, t) &\equiv \int_{-t+t_0}^{t-t_0} d\tau e^{i\Omega\tau} P_{\alpha\beta}(t + \tau, t) \\ &= \frac{1}{2} [C_{\alpha\beta}(\Omega, t) + C_{\alpha\beta}^*(-\Omega, t)], \end{aligned} \quad (37)$$

where  $C_{\alpha\beta}(\Omega, t)$  is the Fourier transform of  $C_{\alpha\beta}(t + \tau, t)$  with respect to  $\tau$ . Note that the relation

$$P_{\alpha\beta}^*(\Omega, t) = P_{\alpha\beta}(-\Omega, t) \quad (38)$$

immediately follows. In Sec. II B, we remarked that it is sufficient for knowledge of  $P_{\alpha\beta}(t_1, t_2)$  to know the nonsymmetrized function  $C_{\alpha\beta}(t_1, t_2)$ .

In addition to the power spectrum, one can calculate several other useful quantities in terms of the  $C_{\alpha\beta}$ . For instance, in a two-lead junction, one may focus on the net current

$$\hat{I}_{LR}^{(-)}(t) = \frac{1}{2}(\hat{I}_L(t) - \hat{I}_R(t)) \quad (39)$$

or on the sum of currents, which by the continuity equation is proportional to the rate of change of charge in the molecule [89]

$$\hat{I}_{LR}^{(+)}(t) = \frac{1}{2}(\hat{I}_L(t) + \hat{I}_R(t)). \quad (40)$$

The time-dependent noise spectra of these objects can be written

$$\begin{aligned} C^{(-)}(\Omega, t) &= \int d\tau e^{i\Omega\tau} \langle \Delta \hat{I}_{LR}^{(-)}(t + \tau) \Delta \hat{I}_{LR}^{(-)}(t) \rangle \\ &= \frac{1}{2}(C^{(\text{auto})}(\Omega, t) - C^{(\times)}(\Omega, t)), \end{aligned} \quad (41)$$

$$\begin{aligned} C^{(+)}(\Omega, t) &= \int d\tau e^{i\Omega\tau} \langle \Delta \hat{I}_{LR}^{(+)}(t + \tau) \Delta \hat{I}_{LR}^{(+)}(t) \rangle \\ &= \frac{1}{2}(C^{(\text{auto})}(\Omega, t) + C^{(\times)}(\Omega, t)), \end{aligned} \quad (42)$$

where we have defined Fourier transforms of the *average* autocorrelation and cross correlations:

$$C^{(\text{auto})}(t + \tau, t) \equiv \frac{1}{2}[C_{LL}(t + \tau, t) + C_{RR}(t + \tau, t)], \quad (43)$$

$$C^{(\times)}(t + \tau, t) \equiv \frac{1}{2}[C_{LR}(t + \tau, t) + C_{RL}(t + \tau, t)]. \quad (44)$$

In general,  $C^{(\text{auto})}$  and  $C^{(\times)}$  are complex quantities and so cannot be observed. However, due to the symmetry property (14), they are both real at the equal observation time point  $\tau = 0$ . This fact was exploited in Ref. [81], where the equal time autocorrelation in the left lead,  $C_{LL}(t, t)$ , was studied in the time domain. Using the identity (14), one can show that the real parts of these functions are always *symmetric* in the  $\tau = 0$  line:

$$\text{Re}[C^{(\text{auto}/\times)}(t + \tau, t)] = \text{Re}[C^{(\text{auto}/\times)}(t, t + \tau)], \quad (45)$$

whereas the imaginary parts are always *antisymmetric* about this line:

$$\text{Im}[C^{(\text{auto}/\times)}(t + \tau, t)] = -\text{Im}[C^{(\text{auto}/\times)}(t, t + \tau)]. \quad (46)$$

To check the validity of our theory, we must confirm that it reduces to known expressions in the long-time and static bias limits, as was already demonstrated for the current in Ref. [88]. We shall assume that the bias is applied only to the leads [ $\varphi_C(t_1, t_2) \equiv 0$ ], that the equilibrium and nonequilibrium effective molecular Hamiltonians are identical ( $\tilde{\mathbf{h}}_{CC}^{\text{eff}} = \mathbf{h}_{CC}^{\text{eff}}$ ), and that  $V_\alpha(t) = V_\alpha$  is constant in time ( $t > t_0$ ). In this case, the  $\mathbf{S}_\alpha$  defined in Eq. (26) can be evaluated explicitly, and in the  $t_0 \rightarrow -\infty$  limit we obtain

$$\mathbf{S}_\gamma(t_1, t_0; \omega) \mathbf{\Gamma}_\gamma \mathbf{S}_\gamma^\dagger(t_2, t_0; \omega) \xrightarrow{t_0 \rightarrow -\infty} e^{-i(\omega + V_\gamma)(t_1 - t_2)} \mathbf{A}_\gamma(\omega + V_\gamma), \quad (47)$$

where  $\mathbf{A}_\gamma(\omega) \equiv \mathbf{G}_{CC}^r(\omega) \mathbf{\Gamma}_\gamma \mathbf{G}_{CC}^a(\omega)$ . Other expressions appearing in the generalized two-time correlation function can be worked out in a similar way, for instance,

$$\begin{aligned} e^{-i\psi_\beta(t_2, t_0)} e^{-i\omega(t_2 - t_0)} \mathbf{S}_\beta^\dagger(t_1, t_0; \omega) \\ \xrightarrow{t_0 \rightarrow -\infty} \mathbf{G}_{CC}^a(\omega + V_\beta) e^{i(\omega + V_\beta)\tau}. \end{aligned} \quad (48)$$

The  $\mathbf{S}_\alpha$  matrices enter into the general expression (36) only in the form of structures like (47) and (48), so we easily conclude that the correlation function  $C_{\alpha\beta}(t_1, t_2)$  depends only on the time difference  $\tau$ , the power spectrum does not depend on time  $t$ . Hence, the current becomes a stationary stochastic



process under the conditions that the bias is static and that the switch-on time is relegated to the distant past. This is implied by the fact that the current itself is simply the steady-state LB formula in this case, as it was proven in Ref. [88] that all terms arising from the initial conditions (vertical contour convolutions) vanish in the long-time limit. With the exception of the initial condition term, every vanishing term includes a convolution with a left or right self-energy. In the partitioned approach to the transport problem, these quantities vanish, as one can see from the definition (7) and the fact that  $\mathbf{h}_{C\alpha}(z) = 0$  for all  $z \in C_M$ .

In studies of high-frequency shot noise, the interesting physical observable is usually the static nonsymmetrized power spectrum [28,31], which is the regular Fourier transform (denoted via  $\mathcal{F}$  hereafter) of  $C_{\alpha\beta}(\tau) \equiv \lim_{t_0 \rightarrow -\infty} C_{\alpha\beta}(t + \tau, t)$ :

$$\begin{aligned} C_{\alpha\beta}(\Omega) &\equiv \lim_{t_0 \rightarrow -\infty} C_{\alpha\beta}(\Omega, t) \\ &= \int_{-\infty}^{\infty} d\tau e^{i\Omega\tau} C_{\alpha\beta}(\tau) \equiv \mathcal{F}[C_{\alpha\beta}(\tau); \Omega]. \end{aligned} \quad (49)$$

$$\begin{aligned} C_{\alpha\alpha}(\Omega) &= 4q^2 \int \frac{d\omega}{2\pi} \text{Tr}_C \left[ [1 - f_{\alpha}(\omega + \Omega - \mu)] f_{\bar{\alpha}}(\omega - \mu) \mathbf{T}_{CC}^{(\alpha\bar{\alpha})}(\omega) \mathbf{T}_{CC}^{\dagger(\alpha\bar{\alpha})}(\omega) \right. \\ &\quad + [1 - f_{\bar{\alpha}}(\omega + \Omega - \mu)] f_{\alpha}(\omega - \mu) \mathbf{T}_{CC}^{(\alpha\bar{\alpha})}(\omega + \Omega) \mathbf{T}_{CC}^{\dagger(\alpha\bar{\alpha})}(\omega + \Omega) \\ &\quad - [f_{\alpha}(\omega - \mu) - f_{\bar{\alpha}}(\omega - \mu)] [f_{\alpha}(\omega + \Omega - \mu) - f_{\bar{\alpha}}(\omega + \Omega - \mu)] \mathbf{T}_{CC}^{(\alpha\bar{\alpha})}(\omega) \mathbf{T}_{CC}^{\dagger(\alpha\bar{\alpha})}(\omega) \mathbf{T}_{CC}^{(\alpha\bar{\alpha})}(\omega + \Omega) \mathbf{T}_{CC}^{\dagger(\alpha\bar{\alpha})}(\omega + \Omega) \\ &\quad \left. + \Omega^2 [1 - f_{\alpha}(\omega + \Omega - \mu)] f_{\alpha}(\omega - \mu) \mathbf{\Gamma}_{\alpha} \mathbf{G}^r(\omega) \mathbf{A}_{\alpha}(\omega + \Omega) \mathbf{G}^a(\omega) \right], \end{aligned} \quad (50)$$

where  $\bar{\alpha} \neq \alpha$ , and we have defined the *transmission matrices* in the standard way [70]:

$$\mathbf{T}_{CC}^{(\alpha\beta)}(\omega) \equiv [\mathbf{\Gamma}_{\alpha}]^{\frac{1}{2}} \mathbf{G}_{CC}^r(\omega) [\mathbf{\Gamma}_{\beta}]^{\frac{1}{2}}, \quad (51)$$

$$\mathbf{T}_{CC}^{\dagger(\alpha\beta)}(\omega) \equiv [\mathbf{\Gamma}_{\beta}]^{\frac{1}{2}} \mathbf{G}_{CC}^a(\omega) [\mathbf{\Gamma}_{\alpha}]^{\frac{1}{2}}. \quad (52)$$

Physically, the eigenvalues of  $\mathbf{T}_{CC}^{(\alpha\beta)}(\omega)$  may be interpreted as probability amplitudes for electron scattering events between the  $\alpha$  and  $\beta$  leads. Equation (50) gives the analytic behavior of a function which should be accessible to the experimentalist: it is a power spectrum for current measurements carried out with arbitrary detection frequency, taken at long times after the switch-on of a constant bias. It is expressed in terms of the transmission matrices, which depend on the molecular Hamiltonian and on the coupling of the molecule to the leads. We remark that if one restricts the  $CC$  region to a single-energy level, and replaces  $\Omega \rightarrow -\Omega$  on the right-hand side, then Eq. (50) is exactly equivalent to the expression found in Ref. [82] (there, the Fourier transform was taken

Note that infinite limits are possible here as  $t_0 \rightarrow -\infty$ . The above quantity satisfies the relation  $C_{\alpha\beta}^*(\Omega) = C_{\beta\alpha}(\Omega)$  [95]. For those experiments which do distinguish between absorption and emission processes, the quantity of interest is most often  $C_{\alpha\alpha}(\Omega)$ , which in general satisfies the inequality  $C_{\alpha\alpha}(\Omega) \neq C_{\alpha\alpha}(-\Omega)$ .  $C_{\alpha\alpha}(\Omega)$  can therefore be used to describe measurements in which a quanta of energy  $\hbar\Omega$  are transferred from the measuring device to the system. By contrast, the symmetrized spectrum obeys  $P_{\alpha\alpha}(\Omega, t) = P_{\alpha\alpha}(-\Omega, t)$ , i.e., it does not distinguish between emission and absorption processes. Moreover, in recently published work [82], a master-equation formalism was used to derive an exact formula for the frequency-dependent autocorrelation and cross-lead current correlations in a nanojunction composed of a quantum dot coupled to two leads, which were treated within the WBLA. In Appendix C, we derive an explicit formula for  $C_{\alpha\beta}(\Omega)$ . Here, we simply note that, if the discussion is restricted to a molecule coupled to left ( $L$ ) and right ( $R$ ) leads, we find that the nonsymmetrized autocorrelation associated with a single lead is given by

with a phase of  $-i\Omega\tau$ ). We note that Ref. [82] also included a numerical scheme for moving beyond the WBLA, and is in this sense more general than the formalism presented in this paper. Indeed, the self-energy in Eq. (D2) contains a singularity at  $t_1 = t_2$ , and appears in Eq. (29) multiplied by  $\delta_{\alpha\beta}$ , so that the autocorrelation function is singular in the two-time plane for  $t_1 = t_2$  whereas the cross-correlation function is finite. This singularity in the autocorrelation is an artifact of the WBLA, and does not exist when the bandwidth of the leads is taken to be finite [81,82]. However, our scheme can be used for rapid calculations on extended molecules with a far larger spectrum than a quantum dot, and in such molecules the WBLA is an increasingly accurate approximation [96,97]. To remove this singularity in the current autocorrelations, one may leave the observation time representation and instead compute the noise in a time-averaged sense. We defer this to a future work and will instead perform calculations of the average cross correlation  $C^{(\times)}(t, t)$  in the  $t$  domain in Sec. IV as this quantity is free from any singularities.

From Eqs. (36) and (15), one obtains the symmetrized two-time correlation function

$$\begin{aligned} P_{\alpha\beta}(t_1, t_2) &= 2q^2 \int \frac{d\omega}{2\pi} \frac{d\omega'}{2\pi} F(\omega, \omega') \text{Tr}_C \left\{ \delta_{\alpha\beta} \sum_{\gamma} (\mathbf{\Gamma}_{\alpha} e^{-i\psi_{\alpha}(t_1, t_2)} e^{-i\omega(t_1 - t_2)} \mathbf{S}_{\gamma}(t_2, t_0; \omega') \mathbf{\Gamma}_{\gamma} \mathbf{S}_{\gamma}^{\dagger}(t_1, t_0; \omega') + \text{H.c.}) \right. \\ &\quad \left. + \sum_{\gamma, \gamma'} \mathbf{\Gamma}_{\alpha} \mathbf{S}_{\gamma}(t_1, t_0; \omega) \mathbf{\Gamma}_{\gamma} \mathbf{S}_{\gamma}^{\dagger}(t_2, t_0; \omega) \mathbf{\Gamma}_{\beta} \mathbf{S}_{\gamma'}(t_2, t_0; \omega') \mathbf{\Gamma}_{\gamma'} \mathbf{S}_{\gamma'}^{\dagger}(t_1, t_0; \omega') \right\} \end{aligned}$$

$$\begin{aligned}
& + i \sum_{\gamma} [\Gamma_{\alpha} \mathbf{S}_{\gamma}(t_1, t_0; \omega) \Gamma_{\gamma} \mathbf{S}_{\gamma}^{\dagger}(t_2, t_0; \omega) \Gamma_{\beta} (e^{-i\psi_{\beta}(t_2, t_0)} e^{-i\omega'(t_2-t_0)} \mathbf{S}_{\beta}^{\dagger}(t_1, t_0; \omega') - e^{i\psi_{\alpha}(t_1, t_0)} e^{i\omega'(t_1-t_0)} \mathbf{S}_{\alpha}(t_2, t_0; \omega')) + \text{H.c.}] \\
& - (e^{-i\psi_{\beta}(t_2, t_0)} e^{-i\omega(t_2-t_0)} \Gamma_{\beta} \mathbf{S}_{\beta}^{\dagger}(t_1, t_0; \omega) e^{-i\psi_{\alpha}(t_1, t_0)} e^{-i\omega'(t_1-t_0)} \Gamma_{\alpha} \mathbf{S}_{\alpha}^{\dagger}(t_2, t_0; \omega') + \text{H.c.}) \Big\}, \tag{53}
\end{aligned}$$

where we define the combination of electron-hole distribution functions:

$$F(\omega, \omega') \equiv [1 - f(\omega - \mu)]f(\omega' - \mu) + [1 - f(\omega' - \mu)]f(\omega - \mu). \tag{54}$$

The steady-state symmetrized power spectrum can then be obtained either by substituting the long-time formulas (47) and (48) into Eq. (53) and taking the Fourier transform, or simply by substituting the expression for  $C_{\alpha\beta}(\Omega)$  into (37):

$$\begin{aligned}
P_{\alpha\beta}(\Omega) \equiv \lim_{t_0 \rightarrow -\infty} P_{\alpha\beta}(\Omega, t) & = 2q^2 \int \frac{d\omega}{2\pi} \left\{ \delta_{\alpha\beta} \sum_{\gamma} \text{Tr}_C [\mathbf{T}_{CC}^{(\alpha\gamma)}(\omega) \mathbf{T}_{CC}^{\dagger(\alpha\gamma)}(\omega)] [F_{\alpha\gamma}(\omega + \Omega, \omega) + F_{\alpha\gamma}(\omega - \Omega, \omega)] \right. \\
& + \sum_{\gamma, \gamma'} F_{\gamma\gamma'}(\omega, \omega - \Omega) \text{Tr}_C [\mathbf{T}_{CC}^{(\alpha\gamma)}(\omega) \mathbf{T}_{CC}^{\dagger(\beta\gamma')}(\omega) \mathbf{T}_{CC}^{(\beta\gamma')}(\omega - \Omega) \mathbf{T}_{CC}^{\dagger(\alpha\gamma')}(\omega - \Omega)] \\
& + i \sum_{\gamma} \text{Tr}_C [\mathbf{T}_{CC}^{(\alpha\gamma)}(\omega) \mathbf{T}_{CC}^{\dagger(\beta\gamma)}(\omega) (F_{\gamma\beta}(\omega, \omega - \Omega) \mathbf{T}_{CC}^{\dagger(\alpha\beta)}(\omega - \Omega) - F_{\gamma\alpha}(\omega, \omega - \Omega) \mathbf{T}_{CC}^{(\beta\alpha)}(\omega - \Omega)) \\
& + \mathbf{T}_{CC}^{(\beta\gamma)}(\omega) \mathbf{T}_{CC}^{\dagger(\alpha\gamma)}(\omega) (F_{\gamma\alpha}(\omega, \omega + \Omega) \mathbf{T}_{CC}^{\dagger(\beta\alpha)}(\omega + \Omega) - F_{\gamma\beta}(\omega, \omega + \Omega) \mathbf{T}_{CC}^{(\alpha\beta)}(\omega + \Omega))] \\
& \left. - \text{Tr}_C [F_{\alpha\beta}(\omega, \omega - \Omega) \mathbf{T}_{CC}^{\dagger(\alpha\beta)}(\omega - \Omega) \mathbf{T}_{CC}^{\dagger(\beta\alpha)}(\omega) + F_{\alpha\beta}(\omega, \omega + \Omega) \mathbf{T}_{CC}^{(\alpha\beta)}(\omega + \Omega) \mathbf{T}_{CC}^{(\beta\alpha)}(\omega)] \right\}, \tag{55}
\end{aligned}$$

where we introduce  $f_{\alpha}(x) \equiv f(x - V_{\alpha})$ , and make the definition

$$F_{\alpha\beta}(\omega, \omega') \equiv [1 - f_{\alpha}(\omega - \mu)]f_{\beta}(\omega' - \mu) + [1 - f_{\beta}(\omega' - \mu)]f_{\alpha}(\omega - \mu) = F_{\beta\alpha}(\omega', \omega).$$

It is instructive to compare this formula with the finite-frequency power spectrum derived by Büttiker and Yang [32–34,47] within their  $S$ -matrix approach. In particular, when one assumes the  $C$  region to be a single level, and there is a Breit-Wigner resonance in the scattering matrix amplitudes of their approach with energy-independent resonance widths [36,37,61], the LB formalism is exactly equivalent to ours. In many experiments, the quantity (55) is measured in the *zero-frequency limit*, i.e., when the time separating measurements is much longer than the time scale over which the current fluctuates [44]. Taking this limit, and using the identity

$$\mathbf{G}_{CC}^r(\omega) = \mathbf{G}_{CC}^a(\omega) - i \sum_{\gamma} \mathbf{G}_{CC}^r(\omega) \Gamma_{\gamma} \mathbf{G}_{CC}^a(\omega), \tag{56}$$

we obtain the zero-frequency power spectrum as

$$\begin{aligned}
\lim_{\Omega \rightarrow 0} P_{\alpha\beta}(\Omega) & = 2q^2 \int \frac{d\omega}{2\pi} \left\{ 2\delta_{\alpha\beta} \sum_{\gamma} F_{\alpha\gamma}(\omega, \omega) \text{Tr}_C [\mathbf{T}_{CC}^{(\alpha\gamma)}(\omega) \mathbf{T}_{CC}^{\dagger(\alpha\gamma)}(\omega)] \right. \\
& - F_{\alpha\beta}(\omega, \omega) \text{Tr}_C [\mathbf{T}_{CC}^{(\alpha\beta)}(\omega) \mathbf{T}_{CC}^{\dagger(\alpha\beta)}(\omega) + \mathbf{T}_{CC}^{(\beta\alpha)}(\omega) \mathbf{T}_{CC}^{\dagger(\beta\alpha)}(\omega)] \\
& + \sum_{\gamma, \gamma'} [F_{\gamma\gamma'}(\omega, \omega) + F_{\alpha\beta}(\omega, \omega)] \text{Tr}_C [\mathbf{T}_{CC}^{(\alpha\gamma)}(\omega) \mathbf{T}_{CC}^{\dagger(\beta\gamma')}(\omega) \mathbf{T}_{CC}^{(\beta\gamma')}(\omega) \mathbf{T}_{CC}^{\dagger(\alpha\gamma')}(\omega)] \\
& + i \sum_{\gamma} \text{Tr}_C [\mathbf{T}_{CC}^{(\alpha\gamma)}(\omega) \mathbf{T}_{CC}^{\dagger(\beta\gamma)}(\omega) (F_{\gamma\beta}(\omega, \omega) \mathbf{T}_{CC}^{\dagger(\alpha\beta)}(\omega) - F_{\gamma\alpha}(\omega, \omega) \mathbf{T}_{CC}^{(\beta\alpha)}(\omega)) \\
& \left. + \mathbf{T}_{CC}^{(\beta\gamma)}(\omega) \mathbf{T}_{CC}^{\dagger(\alpha\gamma)}(\omega) (F_{\gamma\alpha}(\omega, \omega) \mathbf{T}_{CC}^{\dagger(\beta\alpha)}(\omega) - F_{\gamma\beta}(\omega, \omega) \mathbf{T}_{CC}^{(\alpha\beta)}(\omega))] \right\}. \tag{57}
\end{aligned}$$

To better understand the content of the expression (57), we consider the special case where  $\alpha = \beta$ . In this case, use of Eq. (56) enables us to replace the single summation with a double sum, and we can use the identity

$$F_{\alpha\gamma}(\omega, \omega) = \frac{1}{2} [F_{\alpha\alpha}(\omega, \omega) + F_{\gamma\gamma}(\omega, \omega) + 2[f_{\alpha}(\omega - \mu) - f_{\gamma}(\omega - \mu)]^2] \tag{58}$$

to give

$$\lim_{\Omega \rightarrow 0} P_{\alpha\alpha}(\Omega) = P_{\alpha\alpha}^{(\text{thermal})}(\Omega) + P_{\alpha\alpha}^{(\text{shot})}(\Omega), \tag{59}$$

where we identify both the *generalized thermal noise*, which vanishes when the temperature  $T = 0$ , and the *generalized shot noise*, which vanishes when  $V_\gamma = 0$  for all  $\gamma$ :

$$\lim_{\Omega \rightarrow 0} P_{\alpha\alpha}^{(\text{thermal})}(\Omega) = 2q^2 \int \frac{d\omega}{2\pi} \sum_{\gamma \neq \alpha} [F_{\alpha\alpha}(\omega, \omega) + F_{\gamma\gamma}(\omega, \omega)] \text{Tr}_C [\mathbf{T}_{CC}^{(\alpha\gamma)}(\omega) \mathbf{T}_{CC}^{\dagger(\alpha\gamma)}(\omega)], \quad (60)$$

$$\begin{aligned} \lim_{\Omega \rightarrow \infty} P_{\alpha\alpha}^{(\text{shot})}(\Omega) = 2q^2 \int \frac{d\omega}{2\pi} & \left\{ 2 \sum_{\gamma \neq \alpha} [f_\alpha(\omega - \mu) - f_\gamma(\omega - \mu)]^2 \text{Tr}_C \left[ \mathbf{T}_{CC}^{(\alpha\gamma)}(\omega) \mathbf{T}_{CC}^{\dagger(\alpha\gamma)}(\omega) \left( 1 - \sum_{\gamma'} \mathbf{T}_{CC}^{(\alpha\gamma')}(\omega) \mathbf{T}_{CC}^{\dagger(\alpha\gamma')}(\omega) \right) \right] \right. \\ & \left. + \sum_{\gamma, \gamma'} [f_\gamma(\omega - \mu) - f_{\gamma'}(\omega - \mu)]^2 \text{Tr}_C [\mathbf{T}_{CC}^{(\alpha\gamma)}(\omega) \mathbf{T}_{CC}^{\dagger(\alpha\gamma)}(\omega) \mathbf{T}_{CC}^{(\alpha\gamma')}(\omega) \mathbf{T}_{CC}^{\dagger(\alpha\gamma')}(\omega)] \right\}. \quad (61) \end{aligned}$$

If we now specialize this discussion to the case of a two-lead junction, i.e., a junction in which  $\alpha$  may be one of two indices  $L, R$ , we recover the following well-known results for the thermal and shot noise, respectively:

$$\lim_{\Omega \rightarrow 0} P_{LL}^{(\text{thermal})}(\Omega) = 4q^2 \int \frac{d\omega}{2\pi} \{ [1 - f_L(\omega - \mu)] f_L(\omega - \mu) + [1 - f_R(\omega - \mu)] f_R(\omega - \mu) \} \text{Tr}_C [\mathbf{T}_{CC}^{(LR)}(\omega) \mathbf{T}_{CC}^{\dagger(LR)}(\omega)], \quad (62)$$

$$\lim_{\Omega \rightarrow 0} P_{LL}^{(\text{shot})}(\Omega) = 4q^2 \int \frac{d\omega}{2\pi} [f_L(\omega - \mu) - f_R(\omega - \mu)]^2 \text{Tr}_C [\mathbf{T}_{CC}^{(LR)}(\omega) \mathbf{T}_{CC}^{\dagger(LR)}(\omega) (1 - \mathbf{T}_{CC}^{(LR)}(\omega) \mathbf{T}_{CC}^{\dagger(LR)}(\omega))]. \quad (63)$$

Finally, we note that it is common practice [32,70] to neglect the frequency dependence of the transmission functions  $\mathbf{T}_{CC}(\omega) \sim \mathbf{T}_{CC}$  in Eq. (55), which allows for the trivial removal of all frequency integrals. It is then simple to show that the  $LL$  component of Eq. (55) reduces to the well-known expression

$$\begin{aligned} P_{LL}(\Omega) = \frac{q^2}{\pi} & \left\{ \text{Tr}_C [\mathbf{T}_{CC}^{(LR)} \mathbf{T}_{CC}^{\dagger(LR)} \mathbf{T}_{CC}^{(LR)} \mathbf{T}_{CC}^{\dagger(LR)}] 2\Omega \coth \left( \frac{\Omega}{2k_B T} \right) + \text{Tr}_C [\mathbf{T}_{CC}^{(LR)} \mathbf{T}_{CC}^{\dagger(LR)} (1 - \mathbf{T}_{CC}^{(LR)} \mathbf{T}_{CC}^{\dagger(LR)})] \right. \\ & \left. \times \left[ (V_L - V_R - \Omega) \coth \left( \frac{V_L - V_R - \Omega}{2k_B T} \right) + (V_L - V_R + \Omega) \coth \left( \frac{V_L - V_R + \Omega}{2k_B T} \right) \right] \right\}. \quad (64) \end{aligned}$$

This formula expresses the interplay of the shot noise, Nyquist noise, and quantum vacuum fluctuations in a conductor, and moreover has been verified experimentally for a wide range of mesoscale conductors [43,98].

## IV. NUMERICS

### A. Periodic driving bias model

In Appendix D, we present an efficient technique for evaluating each term in Eq. (29) based on the analytical removal of all frequency integrals in these expressions, as was done for the current in Ref. [91]. Other schemes in the literature perform the frequency integrals in the transient noise numerically [81,82], so we acquire a significant computational

speedup in comparison to those works, as well as access to the noise response to an explicit time-dependent driving. Many cases of interest can be studied by inserting into these formulas the following *biharmonic* bias, consisting of a constant shift  $V_\alpha$  and two harmonic modes:

$$\begin{aligned} V_\alpha(t) = V_\alpha + A_\alpha^{(1)} \cos[p_1 \Omega_\alpha (t - t_0) + \phi_\alpha] \\ + A_\alpha^{(2)} \cos[p_2 \Omega_\alpha (t - t_0)]. \quad (65) \end{aligned}$$

Here,  $p_1, p_2$  are any integers and  $\phi_\alpha$  is a lead-dependent phase shift that breaks the dynamical symmetry of the system under time reversal (TR),  $t \rightarrow 2t_0 - t$ . According to a well-known Bessel function identity, this choice of bias leads to the following representation of the exponential phase factor appearing in Eq. (D12):

$$e^{i\psi_\alpha(t_1, t_2)} = e^{iV_\alpha(t_1 - t_2)} \sum_{r, r', s, s'} J_r \left( \frac{A_\alpha^{(1)}}{p_1 \Omega_\alpha} \right) J_{r'} \left( \frac{A_\alpha^{(1)}}{p_1 \Omega_\alpha} \right) J_s \left( \frac{A_\alpha^{(2)}}{p_2 \Omega_\alpha} \right) J_{s'} \left( \frac{A_\alpha^{(2)}}{p_2 \Omega_\alpha} \right) e^{i(r-r')\phi_\alpha} e^{i\Omega_\alpha(p_1 r + p_2 s)(t_1 - t_0)} e^{-i\Omega_\alpha(p_1 r' + p_2 s')(t_2 - t_0)}. \quad (66)$$

In Appendix E, we include explicit formulas for  $\mathbf{G}^{\lessgtr}(t_1, t_2)$  and the  $\mathbf{\Lambda}^\pm$  matrices within this biharmonic model, with all time integrals explicitly removed by hand. In calculations presented here, we will only consider the case of a single harmonic in order to reflect numerical work carried out elsewhere [88,89]. However, the equations presented in this work will be valid for the general biharmonic case studied experimentally in Ref. [59].

### B. Application to the molecular wire

Now, we shall apply our formalism to the transport properties of the molecular wire, using the tight-binding model of a one-dimensional wire with nearest-neighbor hopping from Refs. [99,100]. We previously studied the current response in this system for sinusoidal [89] and stochastic [91] biases in the leads. We assume that each site corresponds to a single-energy level, which may have a maximum occupation of 2 due to

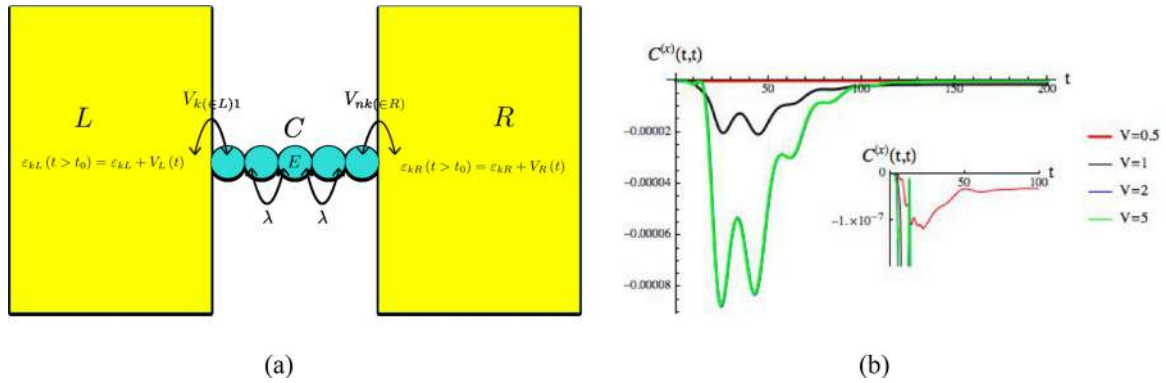


FIG. 1. (a) Schematic of a typical two-lead molecular junction consisting of the left ( $L$ ) and right ( $R$ ) leads bridged by a molecular system  $C$ , which in this case is chosen to be a molecular wire composed of  $N_s = 5$  atomic sites with nearest-neighbor hopping. (b) Plot of  $C^{(\times)}(t, t)$  for the switch-on of a constant bias  $V = V_L = -V_R$ , for the parameter choice  $E = 1$ ,  $\Gamma = 0.5$ ,  $\lambda = 0.1$ .

spin degeneracy, so that our model is equivalent to a wire of coupled quantum dots [101,102]. The Hamiltonian describing this molecular wire is assumed to have onsite energies equal to the constant value  $[\mathbf{h}_{CC}]_{k,k} \equiv E$  and hopping elements all given by  $[\mathbf{h}_{CC}]_{k,k+1} = [\mathbf{h}_{CC}]_{k+1,k} \equiv \lambda$ . All quantities will be given in arbitrary units, and we choose the chemical potential  $\mu = 0$  as the zero of energy. We model the perpendicular orientation of the wire between the leads. In Fig. 1(a), we illustrate the configuration in which only the end sites of the wire are coupled to their neighboring lead, in which case the only nonzero elements of the level width are  $\Gamma_{L,11}$  and  $\Gamma_{R,N_s N_s}$ , where  $N_s$  is the number of molecular sites. For simplicity, we will assume that sites are symmetrically coupled to the left and right leads  $\Gamma_{L,11} = \Gamma/2 = \Gamma_{R,N_s N_s}$ . We will now study the response of the cross correlation in this system to the switch-on of both dc and ac biases.

### 1. Time-dependent response to a dc bias

In Fig. 1(b), we plot the cross correlation  $C^{(\times)}(t, t)$  through a molecular wire for different values of the static ( $A_\alpha^{(1)} = 0 = A_\alpha^{(2)}$ ) bias  $V = V_L = -V_R$ , with  $\Gamma = 0.5$ , onsite energy  $E = 1$ , and the hopping parameter is set to  $\lambda = 0.1$ . In Fig. 1(b), we observe the occurrence of a “kick” in the cross-correlation signal beginning at a resonance time of about  $t_{\text{res}} \simeq 20$ , before the signal decays towards zero. This resonance is extremely small [shown in the inset to Fig. 1(b)] when  $V < E$ , as in this case the onsite energy of the chain lies outside the bias window  $[-V, V]$ . The magnitude of the resonance sharply increases when  $E$  crosses into the bias window at  $V = 1$ , before saturating at a maximum value at around  $V = 2$ , which can be seen from the fact that the  $V = 5$  (green) curve sits almost exactly on top of the  $V = 2$  (blue) one. This resonance is transient; we associate it with the relaxation time taken for the system to reach its steady state.

In Fig. 2 we exhibit the contour plot of  $\text{Re}[C^{(\times)}(t + \tau, t)]$  for the  $V = 5$  case, and for different numbers of atomic sites  $N_s = 3, 4, 5, 6$ . Note that the symmetry property (45) is satisfied in all four plots. Unlike the single-site case in Ref. [82], the magnitude of the cross correlation is *not* in general maximized along the  $\tau = 0$  diagonal. Instead, we see a very strong “ripple” spreading out from the diagonal for all values of  $N_s$  with a maximum magnitude at a value of  $\tau_{\text{max}} = t_1 - t_2$  satisfying

the relation  $\max |\text{Re}[C^{(\times)}(t + \tau, t)]| = \text{Re}[C^{(\times)}(t \pm \tau_{\text{max}}, t)]$ . It appears from Figs. 2(a)–2(d) that  $\tau_{\text{max}}$  increases linearly with increasing  $N_s$ . In the  $N_s = 5$  case  $\tau_{\text{max}} \simeq 20$ , i.e., it is roughly equal to the resonance time  $t_{\text{res}}$  in  $C^{(\times)}(t, t)$ , so we expect that the two time scales  $\tau_{\text{max}}$  and  $t_{\text{res}}$  may be physically related.

The fact that  $\tau_{\text{max}}$  increases with  $N_s$  implies that its position is due to the finite size of the molecular wire and its intrinsic properties. To understand this heuristically, one may consider the Schrödinger equation for a wire of  $N_s$  sites with a spacing of size 1 (i.e., of length  $N_s - 1$ ), energy  $E$ , and intersite coupling  $\lambda$ . This leads to a dispersion  $\varepsilon(k) = E + 2\lambda \cos(k)$ , and therefore the traversal time for an electron of unit mass to pass through the wire is approximated by (note that  $\hbar = 1$ )

$$\tau_{\text{traversal}} \approx \frac{N_s - 1}{\partial_k \varepsilon(k)} = \frac{N_s - 1}{2\lambda \sin(k)}. \quad (67)$$

Whereas this expression neglects the presence of the leads and cannot be taken as anything other than a rule of thumb, it indicates that we may investigate the interplay of  $\lambda$  and  $N_s$  should we wish to understand the effects on the dynamics of a finite system size.

In Figs. 3(b) and 3(d), we show the results of calculations of the absolute value of the Fourier transform of  $\lim_{t_0 \rightarrow -\infty} \text{Re}[C^{(\times)}(t + \tau, t)]$  with respect to  $\tau$ . This is done for each value of  $N_s$  in Fig. 2 by fixing  $t = 2000$  and evaluating a diagonal time slice of each plot shown there for  $\tau \in [-200, 200]$ . These time slices are shown in Figs. 5(a) ( $\lambda = 0.1$ ) and 5(c) ( $\lambda = 0.5$ ). From Eqs. (37) and (49), the quantity plotted in Figs. 3(b) and 3(d) satisfies the following identity:

$$\mathcal{F}[\text{Re}[C^{(\times)}(\tau + t, t)]; \Omega] = \frac{P_{LR}(\Omega) + P_{RL}(\Omega)}{2}. \quad (68)$$

We are therefore simply plotting the absolute value of the average symmetrized cross correlations in Figs. 3(b) and 3(d). In Fig. 3(b), we plot this for  $\lambda = 0.1$ , and observe oscillating resonant frequencies at values of  $n\Omega_{N_s}$  for some intrinsic frequency  $\Omega_{N_s}$  that depends on the length of the wire. We find that  $\Omega_{N_s}$  decreases with increasing wire length. For example, the main  $N_s = 5$  resonance occurs at  $\Omega_5 \simeq 0.15$ , corresponding to a time of  $2\pi/\Omega_5 \simeq 40 \simeq 2\tau_{\text{max}}$ , i.e., the distance between peaks on Figs. 3(a) and 2(b). This is to be expected from the heuristic relation (67) and the contour



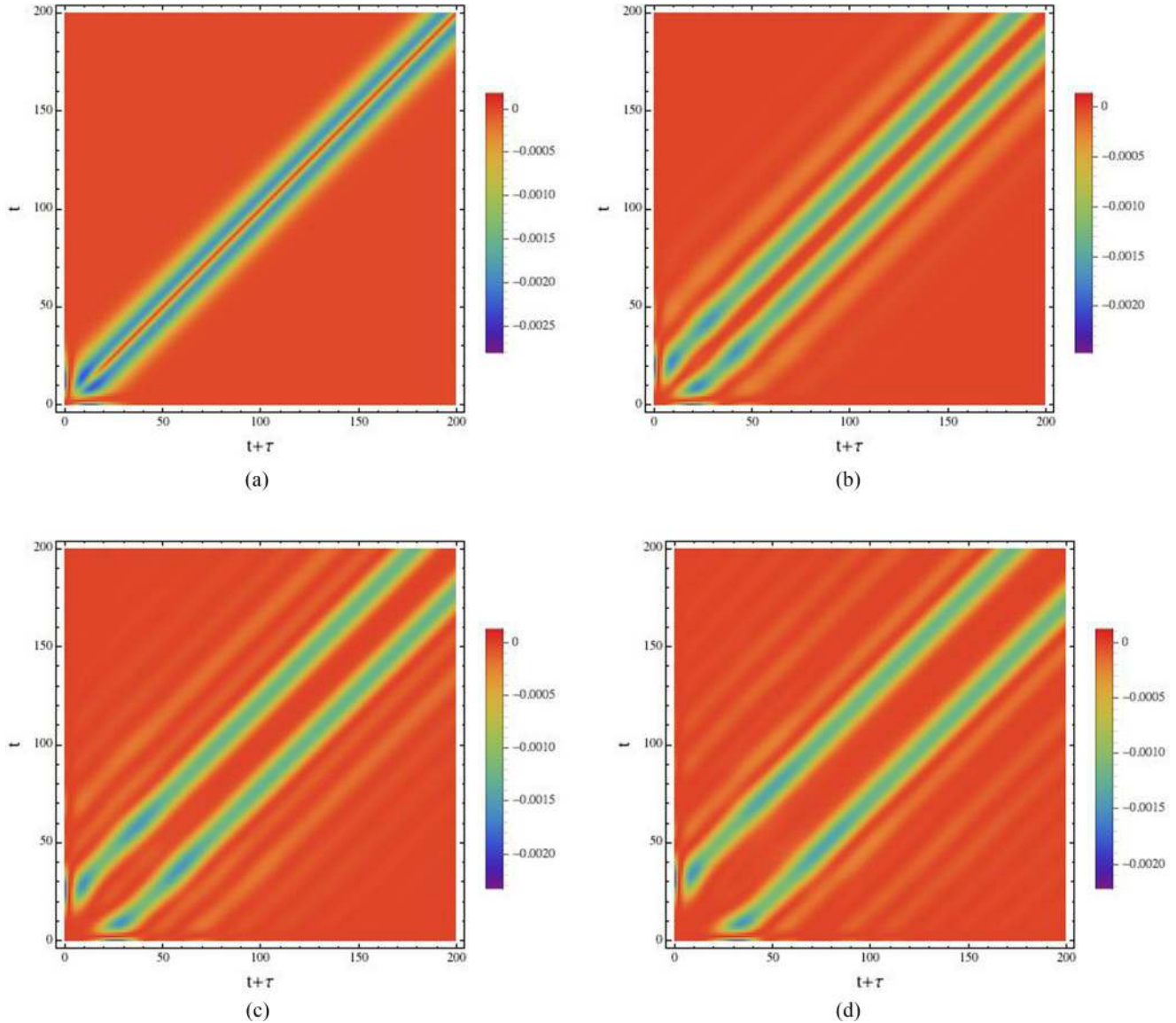


FIG. 2. Plots of  $\text{Re}[C^{(\times)}(t + \tau, t)]$  for  $V = V_L = -V_R = 5$ ,  $\lambda = 0.1$ ,  $E = 1$ ,  $\Gamma = 0.5$  where the number of sites is varied so that (a)  $N_s = 3$ , (b)  $N_s = 4$ , (c)  $N_s = 5$ , and (d)  $N_s = 6$ .

plots of Fig. 2. When we increase the intersite coupling to  $\lambda = 0.5$  in Fig. 3(d), we find that the position of the main resonance, for each value of  $N_s$ , shifts by a factor of roughly 5, so that these peaks can be attributed to wire traversal events. We also see that the higher-frequency modes occurring at multiples of  $\Omega_{N_s}$  are stronger and more numerous in the  $\lambda = 0.5$  case than for  $\lambda = 0.1$ . These modes correspond to the subsidiary “ripples” seen to emanate from the main resonances in Fig. 2. Physically, these ripples are due to internally reflected electrons, or “circular currents” that contribute weakly to the cross-lead correlations in each lead when compared with the main influence of electrons propagating directly from the other lead.

## 2. Time-dependent response to an ac bias

To understand how the time scale of the resonance occurring in the case of the perpendicular wire combines with an ac field, we will now compute the cross correlations for the

same type of driving that was studied in Ref. [89], where long transients were observed due to the relative sparsity of the level width matrix for a wire in the configuration of Fig. 1(a). Specifically, we employ the bias (65)  $V_L = 5$ ,  $V_R = 5$ ,  $A_L^{(1)} = 4 = A_R^{(1)}$ ,  $A_L^{(2)} = 0 = A_R^{(2)}$ ,  $\Omega_L = 1 = \Omega_R \equiv \Omega_D$ , with the only difference between the leads coming from a symmetry-breaking phase:  $\phi_L = 0$ ,  $\phi_R = -\pi/2$ . In Fig. 4(a), we plot the  $\tau = 0$  cross correlation  $C^{(\times)}(t, t)$  for different values of the end-site level width parameter  $\Gamma$  in a five-site wire. Similarly to Fig. 2(a), we observe a resonance occurring in the absolute value of  $C^{(\times)}(t, t)$  for the perpendicular five-site wire at most values of  $\Gamma$ , and the frequency of this resonance, given in Fig. 2(b), does not appear to be related to the driving frequency  $\Omega_D$  as it is unchanged from its position of  $t_{\text{res}} \simeq 20$  in the static bias case considered above in Fig. 1(b). After the resonance, the cross correlation decays to a signal with a smaller amplitude, while retaining a complex periodic “ringing” signal, as shown in the inset to Fig. 4(a). In



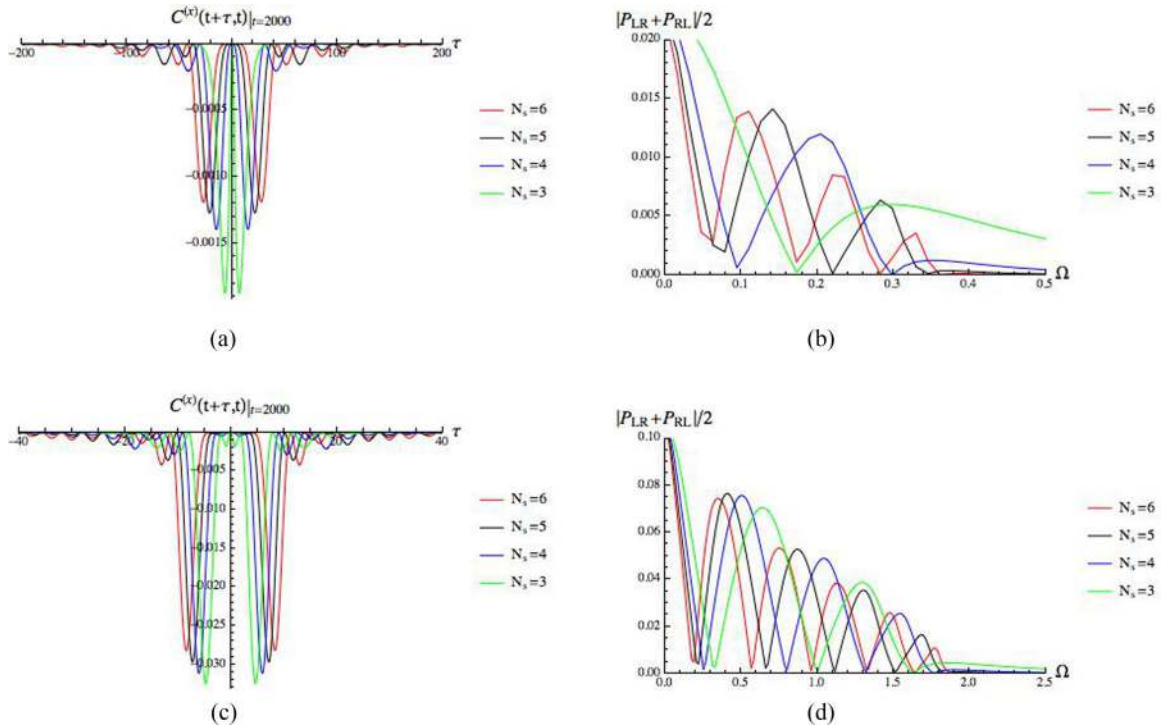


FIG. 3. (a) Cross section of  $\text{Re}[C^{(x)}(t + \tau, t)]_{t=2000}$  for the relative time range  $\tau \in [-200, 200]$ , with  $\lambda = 0.1$ . (b) Plot of the low-frequency end of the average symmetrized power spectrum of cross correlations  $[P_{LR}(\Omega) + P_{RL}(\Omega)]/2$ , obtained as the numerical Fourier transform of the signal in (a). (c) Cross section of  $\text{Re}[C^{(x)}(t + \tau, t)]_{t=2000}$  for the relative time range  $\tau \in [-40, 40]$ , with  $\lambda = 0.5$ . (d) The low-frequency region of  $[P_{LR}(\Omega) + P_{RL}(\Omega)]/2$  obtained from (c). We use the parameters  $V = V_L = -V_R = 5$ ,  $E = 1$ ,  $\Gamma = 0.5$  throughout.

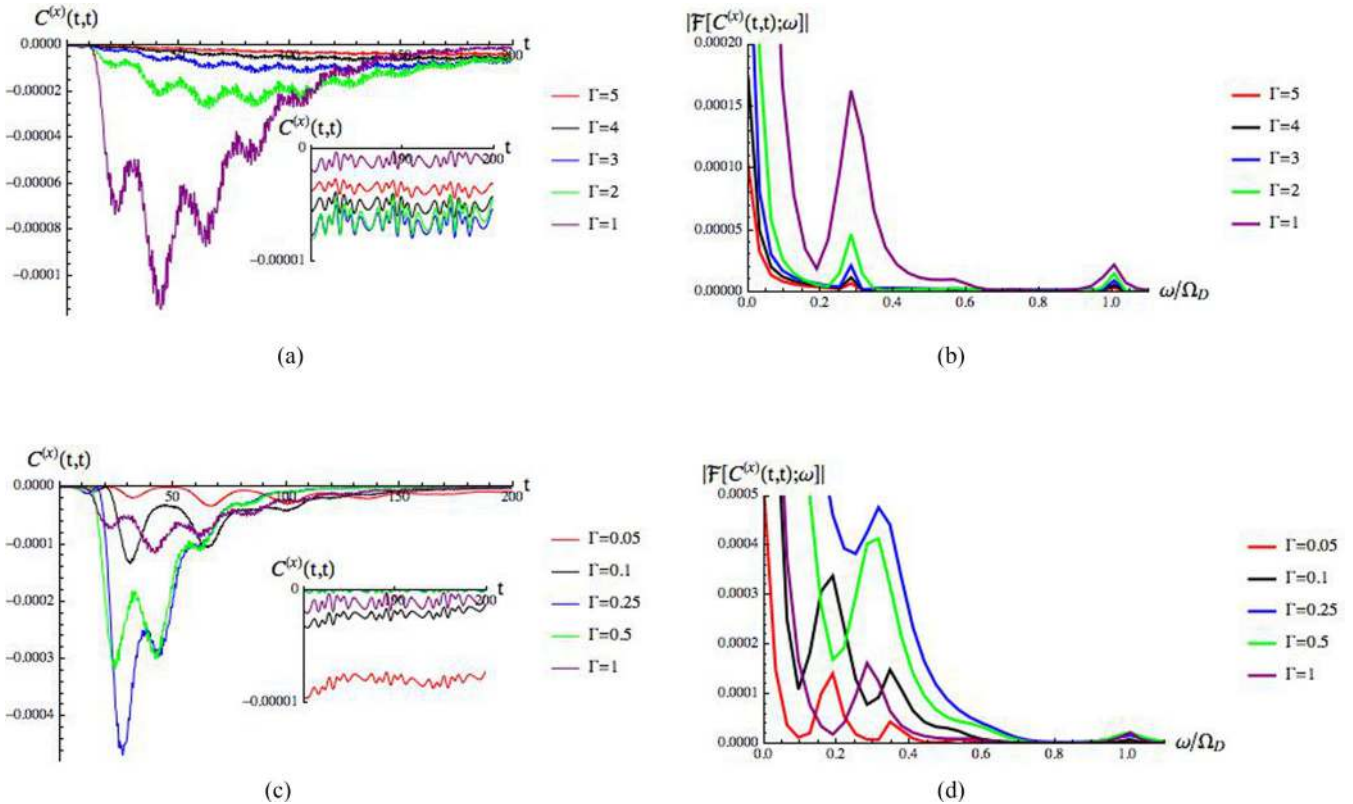


FIG. 4. (a) Plot of  $C^{(x)}(t, t)$  for  $\Gamma \in [1, 5]$ . (b) Plot of the low-frequency end of the absolute value of the Fourier transform  $\mathcal{F}[C^{(x)}(t, t); \omega]$  for the same parameters as (a), in units of the fundamental driving frequency  $\Omega_D$ . (c) Plot of  $C^{(x)}(t, t)$  for  $\Gamma \in [0.05, 1]$ . (d) Plot of the low-frequency end of  $|\mathcal{F}[C^{(x)}(t, t); \omega]|$  for the same parameters as (c). Parameters chosen are  $V_L = 5$ ,  $V_R = 5$ ,  $A_L^{(1)} = 4 = A_R^{(1)}$ ,  $A_L^{(2)} = 0 = A_R^{(2)}$ ,  $\Omega_L = 1 = \Omega_R \equiv \Omega_D$ ,  $\phi_L = 0$ ,  $\phi_R = -\pi/2$ ,  $N_s = 5$ ,  $\lambda = 0.1$ .

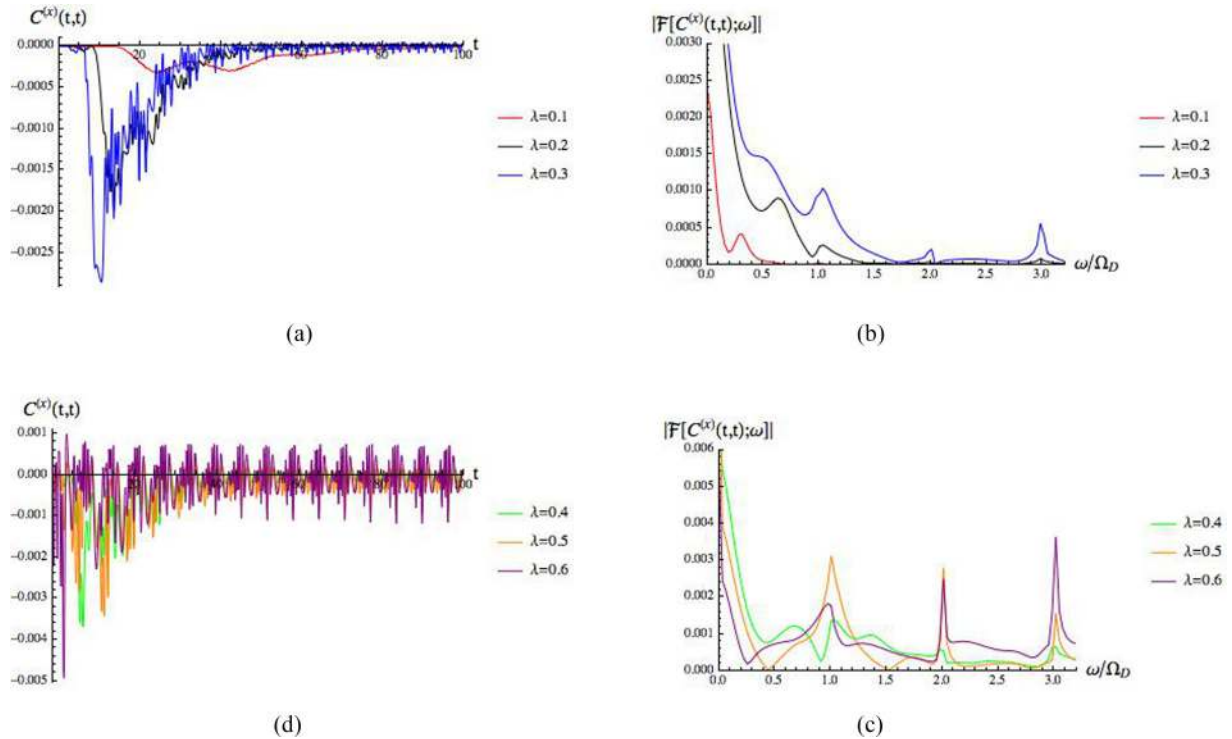


FIG. 5. (a) Plot of  $C^{(\times)}(t,t)$  for  $\lambda \in [0.1, 0.3]$ . (b) Plot of the low-frequency end of the absolute value of the Fourier transform  $\mathcal{F}[C^{(\times)}(t,t); \omega]$  for the same parameters as in (a), in units of the fundamental driving frequency  $\Omega_D$ . (c) Plot of  $C^{(\times)}(t,t)$  for  $\lambda \in [0.4, 0.6]$ . (d) Plot of the low-frequency end of  $|\mathcal{F}[C^{(\times)}(t,t); \omega]|$  for the same parameters as in (c). Parameters chosen are  $V_L = 5$ ,  $V_R = 5$ ,  $A_L^{(1)} = 4 = A_R^{(1)}$ ,  $A_L^{(2)} = 0 = A_R^{(2)}$ ,  $\Omega_L = 1 = \Omega_R \equiv \Omega_D$ ,  $\phi_L = 0$ ,  $\phi_R = -\pi/2$ ,  $N_s = 5$ .

Fig. 4(b), we plot the absolute value of the Fourier transform of the signal in Fig. 4(a) with respect to the *measurement time*, i.e., we compute  $|\mathcal{F}[C^{(\times)}(t,t); \omega]|$ . In addition to the peak at  $\omega = \Omega_D$  corresponding to a regular photon-assisted tunneling process, we observe an additional peak at a much lower frequency, occurring at  $\omega_{\text{res}} \simeq 0.3\Omega_D$ . This frequency should be distinguished from the resonance in the steady-state correlations  $\Omega_N$ : it corresponds to the “kick” that the *diagonal* ( $\tau = 0$ ) cross correlation receives at  $t_{\text{res}} \simeq 20$ , via the relation  $\omega_{\text{res}} = 2\pi/t_{\text{res}}$ . This peak becomes increasingly dominant as  $\Gamma$  is decreased from 5 to 1. In Fig. 4(c), we plot  $C^{(\times)}(t,t)$  for  $\Gamma \in [0.05, 1]$ . It is seen that the resonance at  $\omega_{\text{res}} \simeq 0.3\Omega_D$  continues to grow as  $\Gamma$  decreases, before saturating in the region of  $\Gamma = 0.25$ , whereupon the resonance decays into a less singular form. This is reflected in the frequency spectrum of this signal, shown in Fig. 4(d), which shows how the resonance continues to grow before reaching the saturation value of  $\Gamma$  and splitting into two smaller resonant peaks as  $\Gamma$  tends to 0.

The frequency of the resonance in Figs. 4(b) and 4(d) is located at about  $0.3\text{--}0.35\Omega_D$  regardless of whether the bias is ac or dc, and seems to be only moderately affected by changes in  $\Gamma$ . We therefore suspect that it is due to the finite size and intrinsic properties of the wire. In Fig. 5, we present calculations of the cross correlation in the same system, this time varying the hopping parameter  $\lambda$  and keeping the coupling parameter fixed at  $\Gamma = 0.5$ . Figure 5(a) shows that, as  $\lambda$  is doubled from 0.1 to 0.2, the time at which the resonance kicks in is approximately halved, before being scaled down

by a factor of  $\sim \frac{2}{3}$  as  $\lambda$  is further increased to 0.3. This is reflected in the Fourier transform of these signals shown in Fig. 5(b), which show that the position of the resonant frequency increases linearly with increasing  $\lambda$ , as expected from the heuristic relation (67). As we continue to increase the coupling parameter, the duration of the transient resonance becomes shorter until it approaches the time of  $2\pi$ , i.e., the time period of the fundamental driving frequency  $\omega_{\text{res}} = \Omega_D$  at around  $\lambda = 0.3$ . For values of the coupling greater than this, we see indeed in Fig. 5(c) that that time scale of the transient becomes smaller than the time scale associated with the driving. The frequency spectrum of cross correlations, shown in Fig. 5(d), contains peaks at  $\omega_{\text{res}} \simeq 1.4\Omega_D$  (when  $\lambda = 0.4$ ) and  $\omega_{\text{res}} \simeq 1.75\Omega_D$  (when  $\lambda = 0.5$ ), corresponding to a continuation of the linear dependence of the transient resonant frequency on  $\lambda$ . However, when we cross into the regime of  $\lambda/\Gamma > 1$  (purple line), this resonance has been submerged beneath the growing resonances at integer values of  $\omega/\Omega_D$ , a fact which is reflected in the strongly oscillating signal of the purple line in Fig. 5(c). These resonances continue into the high-frequency part of the spectrum beyond the narrow window exhibited here, and are due to PAT processes.

### 3. Discussion of results

The calculations presented here point to a rather clear physical interpretation of the transient behavior of cross correlations in extended systems. There are three factors which compete to determine how long electrons take to cross the

nanojunction: the strength of the end-site coupling  $\Gamma$ , the length of the wire  $N_s - 1$ , and the internal hopping parameter  $\lambda$ . When  $\Gamma/\lambda > 1$ , the molecular wire is more resistant to propagating electrons than the molecule-electrode interface. Although the large value of  $\Gamma$  tends to reduce the lifetime of molecular modes, the small value of  $\lambda$  makes it difficult for tunneling between sites to occur. This means that the time taken for electrons to traverse the molecular region is significantly longer than the time scale of the external driving field, and so the currents in each lead  $I_L(t)$  and  $I_R(t)$  become more strongly correlated at about the time taken for electrons to propagate between the leads following the switch-on. This explains the resonant kick at  $t_{\text{res}} \simeq 20$  in Figs. 4(a) and 4(c), which remains at this time so long as  $\Gamma > \lambda$ . If  $\lambda$  is kept fixed and  $\Gamma$  is decreased to the weak coupling regime of  $\Gamma/\lambda < 1$ , we enter a regime in which it is energetically easier to tunnel between molecular sites than across the molecule-lead interface. This increases the likelihood of internal reflection or circular currents, and leads to the splitting of the single-frequency peak in Fig. 4(d) into two smaller peaks.

The position of the resonance in frequency space is determined by  $\lambda$  and  $N_s$ . Physically, as the coupling between molecular sites is increased, it becomes increasingly easier for electrons to traverse the wire. In the dc case, we saw that increasing the value of  $\lambda$  increases the strength of reflected currents within the molecular wire. In the ac case, we found that in the regime of  $\lambda \sim \Gamma \sim \Omega_D$ , the time taken for electrons to pass from lead  $L$  to lead  $R$  is smaller than the rate at which photon-assisted electrons tunnel from the lead onto the molecule. In this regime, the electrons can travel between leads in less time than it takes for the signal driving them to undergo an appreciable change.

Once the resonance in  $C^{(\times)}(t, t)$  has died out, a steady state is achieved which is oscillatory in the case of an ac bias and stationary in the case of a dc bias. In the latter case, we saw the emergence of a regime in which each lead at time  $t$  felt the influence of the other most strongly at a time shifted by  $\tau_{\text{max}}$ , which was roughly equal to the time  $t_{\text{res}}$ , and which changed with  $N_s$  and  $\lambda$  in the same way as  $t_{\text{res}}$ . This suggests the existence of a time delay for information to propagate between the  $L$  and  $R$  leads that shows up in the low-frequency power spectrum, and in the equal time cross correlations. The question of how to define the traversal time for electrons tunneling across a nanostructure has been the subject of much debate, with a variety of different definitions proposed, mainly based on the rate of change of wave-packet phase with respect to momentum [103,104]. The results presented here point to a method of determining this time for large molecular structures, namely, by identifying the low-frequency resonances in the transient of  $C^{(\times)}(t, t)$  or in the steady-state Fourier transform of  $C^{(\times)}(t + \tau, t)$  with respect to the time difference  $\tau$ .

## V. CONCLUSIONS

In this paper, we have presented a formalism for the calculation of the time-dependent quantum current correlations in nanojunctions which can be used to study the transient current cross correlations following a partition-free bias switch-on process. The switched-on bias may have any time dependence: our approach is not restricted to periodic or constant biases.

Moreover, our formalism applies to any molecular structure to which the WBLA applies and will be very useful for transport calculations on large molecular structures. Importantly, it perfectly reproduces the steady-state quantum noise formulas obtained previously in Refs. [32,33,82] under the appropriate limits.

We then presented calculations of the cross-lead current correlations both in the full two-time plane and for the equal time ( $\tau = 0$ ) case. Whereas in the single-level case, the magnitude of cross correlations was maximized for a correlation delay time  $\tau_{\text{max}} = 0$ ,  $\tau_{\text{max}}$  was increased significantly with an increase in the number  $N_s$  of atoms in a wire and with decreasing intersite hopping strength  $\lambda$ , so we naturally interpret it as the traversal time for electronic information to cross the nanojunction. In addition, a resonance was observed in the  $\tau = 0$  cross correlation at a time  $t_{\text{res}}$  that could be orders of magnitude greater than the time taken for electrons to tunnel onto the molecule. We found that  $t_{\text{res}}$  was independent of the particular bias chosen but scaled linearly with  $N_s$  and  $1/\lambda$ . This points once again to a signature of the traversal time in the cross correlations. Therefore, we anticipate that our method can be used to determine electron traversal times in a rather more precise way than that offered by heuristic arguments. This will be useful for functional device applications, for example, in determining the maximum operating frequencies in extended molecules used as switches or frequency sensors in real circuits.

We emphasize that we have only begun to explore the parameter space and system size that is now accessible within the biharmonic bias model of Eq. (65). The calculations presented in this paper were intended to complement numerical work done in Refs. [88,89] and therefore only used a single-harmonic driving term. They were also applied to very simple model systems, although our formulas are general and may be applied efficiently to a comparatively larger systems, such as CNT and GNR. In forthcoming work, we will use the method described in Sec. IV to estimate the traversal time for these kinds of structures. We will also show how the formulas presented in Appendix E can be used to achieve ac-dc rectification, or charge pumping, by including the second harmonic in Eq. (65) and manipulating the TR symmetry-breaking phase  $\phi_\alpha$  appearing in the first harmonic.

## ACKNOWLEDGMENTS

We are grateful to R. Tuovinen for his remarks on a preprint of this paper. M.R. was supported through a studentship in the Centre for Doctoral Training on Theory and Simulation of Materials at Imperial College funded by the Engineering and Physical Sciences Research Council under Grant No. EP/G036888/1.

## APPENDIX A: DYSON EQUATIONS FOR MATRIX BLOCKS OF THE GREEN'S FUNCTION

### 1. Lead-molecule coupling terms

In this section, the first and fourth terms in Eq. (19) will be evaluated. First, one utilizes the fact that the Dyson equations for the full  $\alpha - C$  and  $C - \alpha$  Green's functions blocks are

given by

$$\mathbf{G}_{\alpha C}(z_1, z_2) = \int_{\gamma} d\bar{z} \mathbf{g}_{\alpha C}(z_1, \bar{z}) \mathbf{h}_{\alpha C}(\bar{z}) \mathbf{G}_{CC}(\bar{z}, z_2), \quad (\text{A1})$$

$$\mathbf{G}_{C\alpha}(z_1, z_2) = \int_{\gamma} d\bar{z} \mathbf{G}_{CC}(z_1, \bar{z}) \mathbf{h}_{C\alpha}(\bar{z}) \mathbf{g}_{\alpha C}(\bar{z}, z_2). \quad (\text{A2})$$

We now introduce the notation “ $(z_1^-, z_2^+)$ ” to denote that the first argument is always on the upper branch  $C_-$  of the Konstantinov-Perel’ contour, and the second argument always on the lower branch  $C_+$ , and therefore that the second argument is always “later” on the contour than the first. “ $(z_1^+, z_2^-)$ ” denotes the opposite ordering of contour positions, and retaining this ordering is necessary to obtain the correct

initial conditions when the limit  $t_1, t_2 \rightarrow t_0$  is taken. The Langreth rules [93,94] can then be applied to Eqs. (A1) and (A2), which map from the Konstantinov-Perel’ contour onto real and imaginary convolution integrals defined with the following notation:

$$\mathbf{A} \cdot \mathbf{B}(z_1, z_2) \equiv \int_{t_0}^{\infty} d\bar{t} \mathbf{A}(z_1, \bar{t}) \mathbf{B}(\bar{t}, z_2), \quad (\text{A3})$$

$$\mathbf{A} \star \mathbf{B}(z_1, z_2) \equiv -i \int_0^{\beta} d\tau \mathbf{A}(z_1, \tau) \mathbf{B}(\tau, z_2). \quad (\text{A4})$$

This allows us to extract the lesser and greater components of the lead-molecule matrix blocks:

$$\mathbf{G}_{\alpha C}^>(t_1, t_2) = [\mathbf{g}_{\alpha C}^> \mathbf{h}_{\alpha C} \cdot \mathbf{G}_{CC}^a + \mathbf{g}_{\alpha C}^r \mathbf{h}_{\alpha C} \cdot \mathbf{G}_{CC}^> + \mathbf{g}_{\alpha C}^{\leftarrow} \mathbf{h}_{\alpha C} \star \mathbf{G}_{CC}^{\leftarrow}]_{(t_1^+, t_2^-)}, \quad (\text{A5})$$

$$\mathbf{G}_{\beta C}^<(t_2, t_1) = [\mathbf{g}_{\beta C}^< \mathbf{h}_{\beta C} \cdot \mathbf{G}_{CC}^a + \mathbf{g}_{\beta C}^r \mathbf{h}_{\beta C} \cdot \mathbf{G}_{CC}^< + \mathbf{g}_{\beta C}^{\leftarrow} \mathbf{h}_{\beta C} \star \mathbf{G}_{CC}^{\leftarrow}]_{(t_2^-, t_1^+)}, \quad (\text{A6})$$

$$\mathbf{G}_{C\beta}^>(t_1, t_2) = [\mathbf{G}_{CC}^> \cdot \mathbf{h}_{C\beta} \mathbf{g}_{\beta\beta}^a + \mathbf{G}_{CC}^r \cdot \mathbf{h}_{C\beta} \mathbf{g}_{\beta\beta}^> + \mathbf{G}_{CC}^{\leftarrow} \star \mathbf{h}_{C\beta} \mathbf{g}_{\beta\beta}^{\leftarrow}]_{(t_1^+, t_2^-)}, \quad (\text{A7})$$

$$\mathbf{G}_{C\alpha}^<(t_2, t_1) = [\mathbf{G}_{CC}^< \cdot \mathbf{h}_{C\alpha} \mathbf{g}_{\alpha\alpha}^a + \mathbf{G}_{CC}^r \cdot \mathbf{h}_{C\alpha} \mathbf{g}_{\alpha\alpha}^< + \mathbf{G}_{CC}^{\leftarrow} \star \mathbf{h}_{C\alpha} \mathbf{g}_{\alpha\alpha}^{\leftarrow}]_{(t_2^-, t_1^+)}. \quad (\text{A8})$$

These expressions are combined with the definition of the embedding self-energy to give

$$\begin{aligned} & \mathbf{h}_{C\alpha} \mathbf{G}_{\alpha C}^>(t_1, t_2) \mathbf{h}_{C\beta} \mathbf{G}_{\beta C}^<(t_2, t_1) + \mathbf{G}_{C\beta}^>(t_1, t_2) \mathbf{h}_{\beta C} \mathbf{G}_{C\alpha}^<(t_2, t_1) \mathbf{h}_{\alpha C} \\ &= (\Sigma_{\alpha}^> \cdot \mathbf{G}_{CC}^a + \Sigma_{\alpha}^r \cdot \mathbf{G}_{CC}^> + \Sigma_{\alpha}^{\leftarrow} \star \mathbf{G}_{CC}^{\leftarrow})_{(t_1^+, t_2^-)} (\Sigma_{\beta}^< \cdot \mathbf{G}_{CC}^a + \Sigma_{\beta}^r \cdot \mathbf{G}_{CC}^< + \Sigma_{\beta}^{\leftarrow} \star \mathbf{G}_{CC}^{\leftarrow})_{(t_2^-, t_1^+)} \\ &+ (\mathbf{G}_{CC}^> \cdot \Sigma_{\beta}^a + \mathbf{G}_{CC}^r \cdot \Sigma_{\beta}^> + \mathbf{G}_{CC}^{\leftarrow} \star \Sigma_{\beta}^{\leftarrow})_{(t_1^+, t_2^-)} (\mathbf{G}_{CC}^< \cdot \Sigma_{\alpha}^a + \mathbf{G}_{CC}^r \cdot \Sigma_{\alpha}^< + \mathbf{G}_{CC}^{\leftarrow} \star \Sigma_{\alpha}^{\leftarrow})_{(t_2^-, t_1^+)}. \end{aligned} \quad (\text{A9})$$

## 2. Lead-lead and molecule-molecule terms

In this section, the second and third terms in Eq. (19) will be evaluated. The equation of motion (EOM) for the full GF is projected onto the  $\alpha\beta$  region:

$$\left[ i \frac{d}{dz_1} - \mathbf{h}_{\alpha\alpha}(z_1) \right] \mathbf{G}_{\alpha\beta}(z_1, z_2) = \mathbf{I}_{\alpha} \delta_{\alpha\beta} \delta(z_1, z_2) + \mathbf{h}_{\alpha C}(z_1) \mathbf{G}_{C\beta}(z_1, z_2), \quad (\text{A10})$$

$$\mathbf{G}_{\alpha\beta}(z_1, z_2) \left[ -i \frac{\overleftarrow{d}}{dz_2} - \mathbf{h}_{\beta\beta}(z_2) \right] = \mathbf{I}_{\alpha} \delta_{\alpha\beta} \delta(z_1, z_2) + \mathbf{G}_{\alpha C}(z_1, z_2) \mathbf{h}_{C\beta}(z_2). \quad (\text{A11})$$

We insert the fomulas (A1) and (A2) into these EOM to get

$$\left[ i \frac{d}{dz_1} - \mathbf{h}_{\alpha\alpha}(z_1) \right] \mathbf{G}_{\alpha\beta}(z_1, z_2) = \mathbf{I}_{\alpha} \delta_{\alpha\beta} \delta(z_1, z_2) + \int_{\gamma} d\bar{z} \mathbf{h}_{\alpha C}(z_1) \mathbf{G}_{CC}(z_1, \bar{z}) \mathbf{h}_{C\beta}(\bar{z}) \mathbf{g}_{\beta\beta}(\bar{z}, z_2), \quad (\text{A12})$$

$$\mathbf{G}_{\alpha\beta}(z_1, z_2) \left[ -i \frac{\overleftarrow{d}}{dz_2} - \mathbf{h}_{\beta\beta}(z_2) \right] = \mathbf{I}_{\alpha} \delta_{\alpha\beta} \delta(z_1, z_2) + \int_{\gamma} d\bar{z} \mathbf{g}_{\alpha\alpha}(z_1, \bar{z}) \mathbf{h}_{\alpha C}(\bar{z}) \mathbf{G}_{CC}(\bar{z}, z_2) \mathbf{h}_{C\beta}(z_2). \quad (\text{A13})$$

Introducing the GF of the bare leads

$$\left[ i \frac{d}{dz_1} - \mathbf{h}_{\alpha\alpha}(z_1) \right] \mathbf{g}_{\alpha\alpha}(z_1, z_2) = \mathbf{I}_{\alpha} \delta(z_1, z_2), \quad (\text{A14})$$

we can extract the desired Dyson equation

$$\mathbf{G}_{\alpha\beta}(z_1, z_2) = \mathbf{g}_{\alpha\alpha}(z_1, z_2) \delta_{\alpha\beta} + \int_{\gamma} d\bar{z} d\bar{z}' \mathbf{g}_{\alpha\alpha}(z_1, \bar{z}) \mathbf{h}_{\alpha C}(\bar{z}) \mathbf{G}_{CC}(\bar{z}, \bar{z}') \mathbf{h}_{C\beta}(\bar{z}') \mathbf{g}_{\beta\beta}(\bar{z}', z_2). \quad (\text{A15})$$

Once more applying the Langreth rules, the greater and lesser GFs can then be found:

$$\begin{aligned} \mathbf{G}_{\alpha\beta}^>(t_1, t_2) &= \mathbf{g}_{\alpha\alpha}^>(t_1, t_2) \delta_{\alpha\beta} + [(\mathbf{g}_{\alpha\alpha}^> \mathbf{h}_{\alpha C} \cdot \mathbf{G}_{CC}^a + \mathbf{g}_{\alpha\alpha}^r \mathbf{h}_{\alpha C} \cdot \mathbf{G}_{CC}^> + \mathbf{g}_{\alpha\alpha}^{\leftarrow} \mathbf{h}_{\alpha C} \star \mathbf{G}_{CC}^{\leftarrow}) \cdot \mathbf{h}_{C\beta} \mathbf{g}_{\beta\beta}^a \\ &+ \mathbf{g}_{\alpha\alpha}^r \mathbf{h}_{\alpha C} \cdot \mathbf{G}_{CC}^r \cdot \mathbf{h}_{C\beta} \mathbf{g}_{\beta\beta}^> + (\mathbf{g}_{\alpha\alpha}^{\leftarrow} \mathbf{h}_{\alpha C} \cdot \mathbf{G}_{CC}^{\leftarrow} + \mathbf{g}_{\alpha\alpha}^{\leftarrow} \mathbf{h}_{\alpha C} \star \mathbf{G}_{CC}^M) \star \mathbf{h}_{C\beta} \mathbf{g}_{\beta\beta}^{\leftarrow}]_{(t_1^+, t_2^-)}, \end{aligned} \quad (\text{A16})$$

$$\begin{aligned} \mathbf{G}_{\beta\alpha}^<(t_2, t_1) &= \mathbf{g}_{\alpha\alpha}^<(t_2, t_1)\delta_{\alpha\beta} + [(\mathbf{g}_{\beta\beta}^<\mathbf{h}_{\beta C} \cdot \mathbf{G}_{CC}^a + \mathbf{g}_{\beta\beta}^r\mathbf{h}_{\beta C} \cdot \mathbf{G}_{CC}^< + \mathbf{g}_{\beta\beta}^\top\mathbf{h}_{\beta C} \star \mathbf{G}_{CC}^\top) \cdot \mathbf{h}_{C\alpha}\mathbf{g}_{\alpha\alpha}^a \\ &+ \mathbf{g}_{\beta\beta}^r\mathbf{h}_{\beta C} \cdot \mathbf{G}_{CC}^r \cdot \mathbf{h}_{C\alpha}\mathbf{g}_{\alpha\alpha}^< + (\mathbf{g}_{\beta\beta}^r\mathbf{h}_{\beta C} \cdot \mathbf{G}_{CC}^\top + \mathbf{g}_{\beta\beta}^\top\mathbf{h}_{\beta C} \star \mathbf{G}_{CC}^M) \star \mathbf{h}_{C\alpha}\mathbf{g}_{\alpha\alpha}^\top]_{(t_2^-, t_1^+)}. \end{aligned} \quad (\text{A17})$$

We are thus able to write the second and third terms in the correlation function (19) in terms of self-energy and GF components:

$$\begin{aligned} \mathbf{h}_{C\alpha}\mathbf{G}_{\alpha\beta}^>(t_1, t_2)\mathbf{h}_{\beta C} &= \Sigma_\alpha^>(t_1, t_2)\delta_{\alpha\beta} + [(\Sigma_\alpha^> \cdot \mathbf{G}_{CC}^a + \Sigma_\alpha^r \cdot \mathbf{G}_{CC}^> + \Sigma_\alpha^\top \star \mathbf{G}_{CC}^\top) \cdot \Sigma_\beta^a \\ &+ \Sigma_\alpha^r \cdot \mathbf{G}_{CC}^r \cdot \Sigma_\beta^> + (\Sigma_\alpha^r \cdot \mathbf{G}_{CC}^\top + \Sigma_\alpha^\top \star \mathbf{G}_{CC}^M) \star \Sigma_\beta^\top]_{(t_1^+, t_2^-)}, \end{aligned} \quad (\text{A18})$$

$$\begin{aligned} \mathbf{h}_{C\beta}\mathbf{G}_{\beta\alpha}^<(t_2, t_1)\mathbf{h}_{\alpha C} &= \Sigma_\alpha^<(t_2, t_1)\delta_{\alpha\beta} + [(\Sigma_\beta^< \cdot \mathbf{G}_{CC}^a + \Sigma_\beta^r \cdot \mathbf{G}_{CC}^< + \Sigma_\beta^\top \star \mathbf{G}_{CC}^\top) \cdot \Sigma_\alpha^a \\ &+ \Sigma_\beta^r \cdot \mathbf{G}_{CC}^r \cdot \Sigma_\alpha^< + (\Sigma_\beta^r \cdot \mathbf{G}_{CC}^\top + \Sigma_\beta^\top \star \mathbf{G}_{CC}^M) \star \Sigma_\alpha^\top]_{(t_2^-, t_1^+)}. \end{aligned} \quad (\text{A19})$$

To simplify these expressions, we use an identity [68,84]

$$(\Sigma_\alpha^\top \star \mathbf{G}_{CC}^M \star \Sigma_\beta^\top)_{(t_1, t_2)} = 0. \quad (\text{A20})$$

This enables us to neglect the terms in the correlation function arising from a double convolution on  $C_M$  in Eqs. (A18) and (A19), so that in conjunction with Eq. (A9) one finally obtains the correlation function in Eq. (20).

## APPENDIX B: GREEN'S FUNCTIONS AND SELF-ENERGIES FOR THE TIME-DEPENDENT MODEL HAMILTONIAN

We have previously obtained all Green's functions and self-energy components for the switch-on process described by the Hamiltonian in Eq. (2) [91]. We list these below for expediency:

$$\mathbf{G}_{CC}^r(t_1, t_2) = -i\theta(t_1 - t_2)e^{-i\tilde{\mathbf{h}}_{CC}^{\text{eff}}(t_1 - t_2)}e^{-i\varphi_C(t_1, t_2)}, \quad (\text{B1})$$

$$\mathbf{G}_{CC}^a(t_1, t_2) = i\theta(t_2 - t_1)e^{-i(\tilde{\mathbf{h}}_{CC}^{\text{eff}})^\dagger(t_1 - t_2)}e^{-i\varphi_C(t_1, t_2)}, \quad (\text{B2})$$

$$\mathbf{G}_{CC}^M(\tau_1, \tau_2) = \frac{i}{\beta} \sum_{q=-\infty}^{\infty} e^{-\omega_q(\tau_1 - \tau_2)} \begin{cases} (\omega_q - \mathbf{h}_{CC}^{\text{eff}} + \mu)^{-1}, & \text{Im}(\omega_q) > 0 \\ (\omega_q - (\mathbf{h}_{CC}^{\text{eff}})^\dagger + \mu)^{-1}, & \text{Im}(\omega_q) < 0 \end{cases} \quad (\text{B3})$$

$$\mathbf{G}_{CC}^\top(t_1, t_2) = e^{-i\tilde{\mathbf{h}}^{\text{eff}}(t_1 - t_0)}e^{-i\varphi_C(t_1, t_0)} \left[ \mathbf{G}^M(0^+, \tau_2) - i \int_{t_0}^{t_1} d\bar{t} e^{i\tilde{\mathbf{h}}^{\text{eff}}(\bar{t} - t_0)} e^{i\varphi_C(\bar{t}, t_0)} [\Sigma^\top \star \mathbf{G}^M]_{(\bar{t}, \tau_2)} \right],$$

$$\mathbf{G}_{CC}^\top(\tau_1, t_2) = \left[ \mathbf{G}^M(\tau_1, 0^+) + i \int_{t_0}^{\tau_1} d\bar{t} [\mathbf{G}^M \star \Sigma^\top]_{(\tau_1, \bar{t})} e^{-i(\tilde{\mathbf{h}}^{\text{eff}})^\dagger(\bar{t} - t_0)} e^{-i\varphi_C(\bar{t}, t_0)} \right] e^{i(\tilde{\mathbf{h}}^{\text{eff}})^\dagger(t_2 - t_0)} e^{i\varphi_C(t_2, t_0)}, \quad (\text{B4})$$

$$\Sigma_\alpha^r(t_1, t_2) = -\frac{i\Gamma_\alpha}{2} \delta(t_1 - t_2), \quad (\text{B5})$$

$$\Sigma_\alpha^a(t_1, t_2) = \frac{i\Gamma_\alpha}{2} \delta(t_1 - t_2), \quad (\text{B6})$$

$$\Sigma_\alpha^M(\tau_1, \tau_2) = \frac{i}{\beta} \sum_{q=-\infty}^{\infty} e^{-\omega_q(\tau_1 - \tau_2)} \frac{i\Gamma_\alpha}{2} \begin{cases} -1, & \text{Im}(\omega_q) > 0 \\ +1, & \text{Im}(\omega_q) < 0 \end{cases} \quad (\text{B7})$$

$$\Sigma_\alpha^\top(t_1, t_2) = \frac{i\Gamma_\alpha}{\beta} \sum_{q=-\infty}^{\infty} e^{-i\psi_\alpha(t_1, t_0)} e^{\omega_q t_2} \int \frac{d\omega}{2\pi} \frac{e^{-i\omega(t_1 - t_0)}}{\omega_q - \omega + \mu_\alpha}, \quad (\text{B8})$$

$$\Sigma_\alpha^\top(\tau_1, t_2) = \frac{i\Gamma_\alpha}{\beta} \sum_{q=-\infty}^{\infty} e^{-\omega_q \tau_1} e^{i\psi_\alpha(t_2, t_0)} \int \frac{d\omega}{2\pi} \frac{e^{i\omega(t_2 - t_0)}}{\omega_q - \omega + \mu_\alpha}, \quad (\text{B9})$$

$$\Sigma_\alpha^\lessgtr(t_1, t_2) = \pm i\Gamma_\alpha e^{-i\psi_\alpha(t_1, t_2)} \int \frac{d\omega}{2\pi} f[\pm(\omega - \mu)] e^{-i\omega(t_1 - t_2)}. \quad (\text{B10})$$



## APPENDIX C: STEADY-STATE RESULTS

In the limits of long-time and static bias, the general WBLA formula for the two-time correlation given in Eq. (29) may be mapped to the frequency domain as a summation over five terms:

$$C_{\alpha\beta}(\Omega) = \sum_{i=1}^5 C_{\alpha\beta}^{(i)}(\Omega). \quad (\text{C1})$$

The first term is nonzero only when  $\alpha = \beta$ :

$$\begin{aligned} C_{\alpha\beta}^{(1)}(\Omega) &= \lim_{t_0 \rightarrow -\infty, V_\alpha(t) \rightarrow V_\alpha} \int d\tau e^{i\Omega\tau} \delta_{\alpha\beta} 4q^2 \text{Tr}_C[\Sigma_\alpha^>(t_1, t_2) \mathbf{G}_{CC}^<(t_2, t_1) + \mathbf{G}_{CC}^>(t_1, t_2) \Sigma_\alpha^<(t_2, t_1)] \\ &= \delta_{\alpha\beta} 4q^2 \sum_\gamma \int \frac{d\omega}{2\pi} \{ [1 - f_\alpha(\omega + \Omega - \mu)] f_\gamma(\omega - \mu) + [1 - f_\gamma(\omega - \mu)] f_\alpha(\omega - \Omega - \mu) \} T_{\gamma\alpha}(\omega), \end{aligned} \quad (\text{C2})$$

where we have introduced the transmission probability

$$T_{\gamma\alpha}(\omega) \equiv \text{Tr}_C[\mathbf{\Gamma}_\alpha \mathbf{G}^r(\omega) \mathbf{\Gamma}_\gamma \mathbf{G}^a(\omega)]. \quad (\text{C3})$$

Following the interpretative scheme of Ref. [31], we identify the physical origin of this term in processes involving the excitation and propagation of a quasiparticle electron-hole pair, one of which is excited by an energy of  $\hbar\Omega$  with respect to the other. The other terms in  $C_{\alpha\beta}(\Omega)$  occur in higher orders of the level width and involve more complicated electron-hole energy transfer processes:

$$\begin{aligned} C_{\alpha\beta}^{(2)}(\Omega) &= \lim_{t_0 \rightarrow -\infty, V_\alpha(t) \rightarrow V_\alpha} \int d\tau e^{i\Omega\tau} 4q^2 \text{Tr}_C[\mathbf{\Gamma}_\alpha \mathbf{G}_{CC}^>(t + \tau, t) \mathbf{\Gamma}_\beta \mathbf{G}_{CC}^<(t, t + \tau)] \\ &= 4q^2 \sum_{\gamma, \gamma'} \int \frac{d\omega}{2\pi} [1 - f_\gamma(\omega - \mu)] f_{\gamma'}(\omega - \Omega - \mu) \text{Tr}_C[\mathbf{T}_{CC}^{(\alpha\gamma)}(\omega) \mathbf{T}_{CC}^{\dagger(\beta\gamma)}(\omega) \mathbf{T}_{CC}^{(\beta\gamma')}(\omega - \Omega) \mathbf{T}_{CC}^{\dagger(\alpha\gamma')}(\omega - \Omega)], \end{aligned} \quad (\text{C4})$$

$$\begin{aligned} C_{\alpha\beta}^{(3)}(\Omega) &= \lim_{t_0 \rightarrow -\infty, V_\alpha(t) \rightarrow V_\alpha} \int d\tau e^{i\Omega\tau} i 4q^2 \text{Tr}_C[\mathbf{G}_{CC}^>(t + \tau, t) [\mathbf{\Lambda}_\beta^+(t, t + \tau) \mathbf{\Gamma}_\alpha + \mathbf{\Gamma}_\beta (\mathbf{\Lambda}_\alpha^+)^\dagger(t + \tau, t)]] \\ &= i 4q^2 \sum_\gamma \int \frac{d\omega}{2\pi} \text{Tr}_C[[1 - f_\gamma(\omega - \mu)] f_\beta(\omega - \Omega - \mu) \mathbf{A}_\gamma(\omega) \mathbf{\Gamma}_\beta \mathbf{G}_{CC}^a(\omega - \Omega) \mathbf{\Gamma}_\alpha \\ &\quad - [1 - f_\gamma(\omega - \mu)] f_\alpha(\omega - \Omega - \mu) \mathbf{A}_\gamma(\omega) \mathbf{\Gamma}_\beta \mathbf{G}_{CC}^r(\omega - \Omega) \mathbf{\Gamma}_\alpha], \end{aligned} \quad (\text{C5})$$

$$\begin{aligned} C_{\alpha\beta}^{(4)}(\Omega) &= \lim_{t_0 \rightarrow -\infty, V_\alpha(t) \rightarrow V_\alpha} \int d\tau e^{i\Omega\tau} i 4q^2 \text{Tr}_C\{[\mathbf{\Lambda}_\alpha^-(t + \tau, t) \mathbf{\Gamma}_\beta + \mathbf{\Gamma}_\alpha (\mathbf{\Lambda}_\beta^-)^\dagger(t, t + \tau)] \mathbf{G}_{CC}^<(t, t + \tau)\} \\ &= i 4q^2 \sum_\gamma \int \frac{d\omega}{2\pi} \text{Tr}_C[[1 - f_\alpha(\omega - \mu)] f_\gamma(\omega - \Omega - \mu) \mathbf{\Gamma}_\alpha \mathbf{G}_{CC}^a(\omega) \mathbf{\Gamma}_\beta \mathbf{A}_\gamma(\omega - \Omega) \\ &\quad - [1 - f_\beta(\omega - \mu)] f_\gamma(\omega - \Omega - \mu) \mathbf{\Gamma}_\alpha \mathbf{G}_{CC}^r(\omega) \mathbf{\Gamma}_\beta \mathbf{A}_\gamma(\omega - \Omega)], \end{aligned} \quad (\text{C6})$$

$$\begin{aligned} C_{\alpha\beta}^{(5)}(\Omega) &= \lim_{t_0 \rightarrow -\infty, V_\alpha(t) \rightarrow V_\alpha} - \int d\tau e^{i\Omega\tau} i 4q^2 \text{Tr}_C[\mathbf{\Lambda}_\beta^+(t, t + \tau) \mathbf{\Lambda}_\alpha^-(t + \tau, t) + (\mathbf{\Lambda}_\alpha^+)^\dagger(t + \tau, t) (\mathbf{\Lambda}_\beta^-)^\dagger(t, t + \tau)] \\ &= -4q^2 \sum_\gamma \int \frac{d\omega}{2\pi} \text{Tr}_C[f_\beta(\omega - \Omega - \mu) [1 - f_\alpha(\omega - \mu)] \mathbf{\Gamma}_\alpha \mathbf{G}_{CC}^a(\omega) \mathbf{\Gamma}_\beta \mathbf{G}_{CC}^a(\omega - \Omega) \\ &\quad + f_\alpha(\omega - \Omega - \mu) [1 - f_\beta(\omega - \mu)] \mathbf{\Gamma}_\alpha \mathbf{G}_{CC}^r(\omega) \mathbf{\Gamma}_\beta \mathbf{G}_{CC}^r(\omega - \Omega)]. \end{aligned} \quad (\text{C7})$$

These formulas are then substituted into Eq. (C1) to get (50) after some lengthy algebra.

## APPENDIX D: FORMULAS FOR A FAST NUMERICAL IMPLEMENTATION

In this Appendix, we provide exact formulas for all terms appearing in Eq. (29). Our method is based on the fact that we can expand the Fermi function into a series expansion whose terms possess a simple pole structure [105]:

$$f(x) = \frac{1}{e^{\beta x} + 1} = \frac{1}{2} - \lim_{N_p \rightarrow \infty} \sum_{l=1}^{N_p} \eta_l \left( \frac{1}{\beta x + i \zeta_l} + \frac{1}{\beta x - i \zeta_l} \right). \quad (\text{D1})$$

When the parameter values are  $\eta_l = 1$  and  $\zeta_l = \pi(2l - 1)$ , this is referred to as the Matsubara expansion, but one can also improve the convergence of this series for finite  $N_p$  by expressing the Fermi function as a finite continued fraction, and then poles

of the Fermi function can be found as the solution to an eigenproblem for a tridiagonal matrix [106–108]. From the Matsubara expansion, one can write the lesser/greater self-energies as follows:

$$\Sigma_{\alpha}^{\lessgtr}(t_1, t_2) = \pm i \frac{\Gamma_{\alpha}}{2} \delta(t_1 - t_2) - \Gamma_{\alpha} e^{-i\psi_{\alpha}(t_1, t_2)} e^{-i\mu(t_1 - t_2)} \operatorname{cosech} \left( \frac{\pi}{\beta} (t_1 - t_2) \right) \Big|_{t_1 \neq t_2}, \quad (\text{D2})$$

where we define  $\operatorname{cosech}(\frac{\pi}{\beta}(t_1 - t_2))|_{t_1 \neq t_2}$  such that it is equal to zero when  $t_1 = t_2$ . In practice, this function is implemented using the Padé parameters as in Ref. [89]:

$$\operatorname{cosech} \left( \frac{\pi}{\beta} (t_1 - t_2) \right) \Big|_{t_1 \neq t_2} \simeq 2 \sum_{l=1}^{N_p} \eta_l \left[ \theta(t_1 - t_2) e^{-\frac{\eta_l}{\beta}(t_1 - t_2)} - \theta(t_2 - t_1) e^{-\frac{\eta_l}{\beta}(t_2 - t_1)} \right], \quad (\text{D3})$$

where the step function is defined by the midpoint convention:

$$\theta(x) = \begin{cases} 1, & x > 0 \\ \frac{1}{2}, & x = 0 \\ 0, & x < 0. \end{cases} \quad (\text{D4})$$

This evaluation in Eq. (D3) is extremely precise at large  $t_1 - t_2$ , but diverges less rapidly than the true cosech at  $t_1 \sim t_2$ , thus avoiding numerical errors in the integration. We remark that the delta function in the first term of Eq. (D2) is the reason for the divergence in the current autocorrelation at  $t_1 = t_2$  in the WBLA.

The effective Hamiltonian  $\mathbf{h}_{CC}^{\text{eff}}$  is non-Hermitian. We introduce the left and right eigenvectors of this, which are known to share the same eigenvalues [85]:

$$\mathbf{h}_{CC}^{\text{eff}} |\varphi_j^R\rangle = \bar{\varepsilon}_j |\varphi_j^R\rangle \quad \text{and} \quad \langle \varphi_j^L | \mathbf{h}_{CC}^{\text{eff}} = \bar{\varepsilon}_j \langle \varphi_j^L|. \quad (\text{D5})$$

By inserting the expansion in Eq. (D1) and removing all frequency integrals, it is possible to evaluate exactly the  $\Lambda^{\pm}$  matrices defined in Eqs. (34) and (35) in terms of the so-called *Hurwitz-Lerch transcendent*  $\Phi$  [109]:

$$\Phi(z, s, a) \equiv \sum_{n=0}^{\infty} \frac{z^n}{(n+a)^s}. \quad (\text{D6})$$

This arises from integrals over terms of the form  $e^{i\omega\tau}/(\omega - z)$ , where  $z$  is a complex-valued pole. Thus, we derive expressions for the  $\Lambda^{\pm}$  matrices in the left/right eigenbasis and with all frequency integrals removed:

$$\Lambda_{\beta}^{+}(t_2, t_1) = \sum_j \frac{\Gamma_{\beta} |\varphi_j^L\rangle \langle \varphi_j^R|}{\langle \varphi_j^R | \varphi_j^L \rangle} \left[ -\frac{i}{2\beta} \int_{t_0}^{t_1} d\tau e^{i\bar{\varepsilon}_j^*(t_1 - \tau)} e^{-i\mu(t_2 - \tau)} e^{-i\psi_{\beta}(t_2, \tau)} \operatorname{cosech} \left( \frac{\pi}{\beta} (t_2 - \tau) \right) \Big|_{t_2 \neq \tau} \right. \\ \left. - \theta(t_1 - t_2) \frac{e^{i\bar{\varepsilon}_j^*(t_1 - t_2)}}{2} - \frac{i}{2\pi} e^{i\bar{\varepsilon}_j^*(t_1 - t_0)} e^{-i\mu(t_2 - t_0)} e^{-i\psi_{\beta}(t_2, t_0)} \bar{\Phi}(\beta, t_2 - t_0, \bar{\varepsilon}_j^* - \mu) \right], \quad (\text{D7})$$

$$(\Lambda_{\alpha}^{+})^{\dagger}(t_1, t_2) = \sum_j \frac{|\varphi_j^R\rangle \langle \varphi_j^L| \Gamma_{\alpha}}{\langle \varphi_j^L | \varphi_j^R \rangle} \left[ \frac{i}{2\beta} \int_{t_0}^{t_2} d\tau e^{-i\bar{\varepsilon}_j(t_2 - \tau)} e^{i\mu(t_1 - \tau)} e^{i\psi_{\alpha}(t_1, \tau)} \operatorname{cosech} \left( \frac{\pi}{\beta} (t_1 - \tau) \right) \Big|_{t_1 \neq \tau} \right. \\ \left. - \theta(t_2 - t_1) \frac{e^{-i\bar{\varepsilon}_j(t_2 - t_1)}}{2} + \frac{i}{2\pi} e^{-i\bar{\varepsilon}_j(t_2 - t_0)} e^{i\mu(t_1 - t_0)} e^{i\psi_{\alpha}(t_1, t_0)} \bar{\Phi}[\beta, t_1 - t_0, -(\bar{\varepsilon}_j - \mu)] \right], \quad (\text{D8})$$

$$\Lambda_{\alpha}^{-}(t_1, t_2) = \sum_j \frac{\Gamma_{\alpha} |\varphi_j^L\rangle \langle \varphi_j^R|}{\langle \varphi_j^R | \varphi_j^L \rangle} \left[ -\frac{i}{2\beta} \int_{t_0}^{t_2} d\tau e^{i\bar{\varepsilon}_j^*(t_2 - \tau)} e^{-i\mu(t_1 - \tau)} e^{-i\psi_{\alpha}(t_1, \tau)} \operatorname{cosech} \left( \frac{\pi}{\beta} (t_1 - \tau) \right) \Big|_{t_1 \neq \tau} \right. \\ \left. + \theta(t_2 - t_1) \frac{e^{i\bar{\varepsilon}_j^*(t_2 - t_1)}}{2} - \frac{i}{2\pi} e^{i\bar{\varepsilon}_j^*(t_2 - t_0)} e^{-i\mu(t_1 - t_0)} e^{-i\psi_{\alpha}(t_1, t_0)} \bar{\Phi}(\beta, t_1 - t_0, \bar{\varepsilon}_j^* - \mu) \right], \quad (\text{D9})$$

$$(\Lambda_{\beta}^{-})^{\dagger}(t_2, t_1) = \sum_j \frac{|\varphi_j^R\rangle \langle \varphi_j^L| \Gamma_{\beta}}{\langle \varphi_j^L | \varphi_j^R \rangle} \left[ \frac{i}{2\beta} \int_{t_0}^{t_1} d\tau e^{-i\bar{\varepsilon}_j(t_1 - \tau)} e^{i\mu(t_2 - \tau)} e^{i\psi_{\beta}(t_2, \tau)} \operatorname{cosech} \left( \frac{\pi}{\beta} (t_2 - \tau) \right) \Big|_{t_2 \neq \tau} \right. \\ \left. + \theta(t_1 - t_2) \frac{e^{-i\bar{\varepsilon}_j(t_1 - t_2)}}{2} + \frac{i}{2\pi} e^{-i\bar{\varepsilon}_j(t_1 - t_0)} e^{i\mu(t_2 - t_0)} e^{i\psi_{\beta}(t_2, t_0)} \bar{\Phi}[\beta, t_2 - t_0, -(\bar{\varepsilon}_j - \mu)] \right]. \quad (\text{D10})$$

Here, we have defined the following compact object in terms of the Hurwitz-Lerch transcendent:

$$\bar{\Phi}(\beta, \tau, z) \equiv \exp \left( -\frac{\pi}{\beta} \tau \right) \Phi \left( e^{-\frac{2\pi\tau}{\beta}}, 1, \frac{1}{2} + \frac{\beta z}{2i\pi} \right). \quad (\text{D11})$$

In addition, the lesser and greater Green's functions can be put into a convenient form for the numerical evaluation:

$$\begin{aligned}
\mathbf{G}_{CC}^{\geq}(t_1, t_2) = & \frac{1}{2\pi} \sum_{\gamma, k, j} \frac{|\varphi_j^R\rangle\langle\varphi_j^L| \Gamma_{\gamma} |\varphi_k^L\rangle\langle\varphi_k^R|}{\langle\varphi_j^L|\varphi_j^R\rangle\langle\varphi_k^R|\varphi_k^L\rangle} e^{-i\varphi_c(t_1, t_2)} e^{-i\bar{\varepsilon}_j(t_1 - t_0)} e^{i\bar{\varepsilon}_k^*(t_2 - t_0)} \\
& \times \left\{ \frac{i}{\bar{\varepsilon}_k^* - \bar{\varepsilon}_j} \left[ \Psi\left(\frac{1}{2} + \frac{\beta}{2i\pi}(\bar{\varepsilon}_k^* - \mu)\right) - \Psi\left(\frac{1}{2} - \frac{\beta}{2i\pi}(\bar{\varepsilon}_j - \mu)\right) \right] \right. \\
& \pm \frac{\pi}{\bar{\varepsilon}_k^* - \bar{\varepsilon}_j} \left[ \theta(t_1 - t_2) e^{i(\bar{\varepsilon}_j - \bar{\varepsilon}_k^*)(t_2 - t_0)} + \theta(t_2 - t_1) e^{i(\bar{\varepsilon}_j - \bar{\varepsilon}_k^*)(t_1 - t_0)} \right] \\
& - \left( \int_{t_0}^{t_1} d\tau e^{i(\bar{\varepsilon}_j - \mu)(\tau - t_0)} e^{i(\varphi_c - \psi_{\gamma})(\tau, t_0)} \bar{\Phi}(\beta, \tau - t_0, \bar{\varepsilon}_k^* - \mu) - \text{c.c.}_{j \leftrightarrow k, t_1 \leftrightarrow t_2} \right) \\
& - \frac{2\pi}{\beta} [\theta(t_1 - t_2) I(t_2, \beta, \mu, \bar{\varepsilon}_j, \bar{\varepsilon}_k^*) + \theta(t_2 - t_1) I(t_1, \beta, \mu, \bar{\varepsilon}_j, \bar{\varepsilon}_k^*)] \\
& \left. - \frac{2\pi}{\beta} \sum_l \eta_l \left[ \theta(t_1 - t_2) \int_{t_2}^{t_1} d\tau \int_{t_0}^{t_2} d\bar{\tau} e^{i(\bar{\varepsilon}_j - \mu + i\frac{\zeta_l}{\beta})(\tau - t_0)} e^{-i(\bar{\varepsilon}_k^* - \mu + i\frac{\zeta_l}{\beta})(\bar{\tau} - t_0)} e^{i(\varphi_c - \psi_{\gamma})(\tau, \bar{\tau})} - \text{c.c.}_{j \leftrightarrow k, t_1 \leftrightarrow t_2} \right] \right\}, \quad (\text{D12})
\end{aligned}$$

where  $\text{c.c.}_{j \leftrightarrow k, t_1 \leftrightarrow t_2}$  denotes the complex conjugation of the preceding term with both the  $j$  and  $k$  indices and the times  $t_1$  and  $t_2$  exchanged, and we have defined the function

$$I(t, \beta, \mu, \bar{\varepsilon}_j, \bar{\varepsilon}_k^*) = \int_{t_0}^t d\tau \int_{t_0}^t d\bar{\tau} e^{i(\bar{\varepsilon}_j - \mu)(\tau - t_0)} e^{-i(\bar{\varepsilon}_k^* - \mu)(\bar{\tau} - t_0)} e^{i(\varphi_c - \psi_{\gamma})(\tau, \bar{\tau})} \text{cosech}\left(\frac{\pi}{\beta}(\tau - \bar{\tau})\right) \Big|_{\tau \neq \bar{\tau}}. \quad (\text{D13})$$

Here, we have introduced the *digamma function*  $\Psi$ , defined as the logarithmic derivative of the complex gamma function  $\Psi(z) \equiv \frac{d \ln \Gamma(z)}{dz}$  [76]. Note that we can get  $\mathbf{G}^<$  directly from  $\mathbf{G}^>$  on each summation cycle via the following useful property:

$$\mathbf{G}^>(t_1, t_2) - \mathbf{G}^<(t_1, t_2) = -i e^{-i\varphi_c(t_1, t_2)} \sum_j \left[ \frac{|\varphi_j^R\rangle\langle\varphi_j^L|}{\langle\varphi_j^L|\varphi_j^R\rangle} e^{-i\bar{\varepsilon}_j(t_1 - t_2)} \theta(t_1 - t_2) + \frac{|\varphi_j^L\rangle\langle\varphi_j^R|}{\langle\varphi_j^R|\varphi_j^L\rangle} e^{i\bar{\varepsilon}_j^*(t_2 - t_1)} \theta(t_2 - t_1) \right]. \quad (\text{D14})$$

This means a single nested loop of calculations in the two-time plane is sufficient to calculate both Green's functions. We then use the fact that  $\mathbf{G}^<(t_1, t_2) = -\mathbf{G}^<(t_2, t_1)^\dagger$  to get the time-reversed GFs, thus further reducing the calculation time by a half.

## APPENDIX E: FORMULAS FOR THE GREEN'S FUNCTIONS AND LAMBDA MATRICES IN THE BIHARMONIC MODEL

When we substitute Eq. (66) into Eq. (D12), we obtain the following result for the greater and lesser Green's functions:

$$\begin{aligned}
\mathbf{G}^{\geq}(t_1, t_2) = & \frac{1}{2\pi} \sum_{\gamma, k, j} \frac{|\varphi_j^R\rangle\langle\varphi_j^L| \Gamma_{\gamma} |\varphi_k^L\rangle\langle\varphi_k^R|}{\langle\varphi_j^L|\varphi_j^R\rangle\langle\varphi_k^R|\varphi_k^L\rangle} \left\{ \pm \frac{\pi}{\bar{\varepsilon}_k^* - \bar{\varepsilon}_j} [\theta(t_1 - t_2) e^{-i\bar{\varepsilon}_j(t_1 - t_2)} + \theta(t_2 - t_1) e^{i\bar{\varepsilon}_k^*(t_2 - t_1)}] \right. \\
& + \frac{i e^{-i\bar{\varepsilon}_j(t_1 - t_0)} e^{i\bar{\varepsilon}_k^*(t_2 - t_0)}}{\bar{\varepsilon}_k^* - \bar{\varepsilon}_j} \left[ \Psi\left(\frac{1}{2} + \frac{\beta}{2i\pi}(\bar{\varepsilon}_k^* - \mu)\right) - \Psi\left(\frac{1}{2} - \frac{\beta}{2i\pi}(\bar{\varepsilon}_j - \mu)\right) \right] \\
& + i \sum_{r, s} J_r \left( \frac{A_{\gamma}^{(1)}}{p_1 \Omega_{\gamma}} \right) J_s \left( \frac{A_{\gamma}^{(2)}}{p_2 \Omega_{\gamma}} \right) \left[ \frac{e^{-ir\phi_{\gamma}} e^{i\frac{A_{\gamma}^{(1)}}{p_1 \Omega_{\gamma}} \sin \phi_{\gamma}}}{\bar{\varepsilon}_j - \bar{\varepsilon}_k^* - V_{\gamma} - \Omega_{\gamma}(p_1 r + p_2 s)} \right. \\
& \times \left[ e^{-i\bar{\varepsilon}_j(t_1 - t_0)} e^{i\bar{\varepsilon}_k^*(t_2 - t_0)} \left[ \Psi\left(\frac{1}{2} + \frac{\beta}{2\pi i}(\bar{\varepsilon}_k^* - \mu)\right) - \Psi\left(\frac{1}{2} + \frac{\beta}{2\pi i}(\bar{\varepsilon}_j - \mu - V_{\gamma} - \Omega_{\gamma}(p_1 r + p_2 s))\right) \right] \right. \\
& \left. \left. + e^{i\bar{\varepsilon}_k^*(t_2 - t_0)} e^{-i(\mu + V_{\gamma} + \Omega_{\gamma}(p_1 r + p_2 s))(t_1 - t_0)} [\bar{\Phi}(t_1 - t_0, \beta, \bar{\varepsilon}_k^* - \mu) - \bar{\Phi}(t_1 - t_0, \beta, \bar{\varepsilon}_j - \mu - V_{\gamma} - \Omega_{\gamma}(p_1 r + p_2 s))] \right] \right. \\
& + \frac{e^{ir\phi_{\gamma}} e^{-i\frac{A_{\gamma}^{(1)}}{p_1 \Omega_{\gamma}} \sin \phi_{\gamma}}}{\bar{\varepsilon}_k^* - \bar{\varepsilon}_j - V_{\gamma} - \Omega_{\gamma}(p_1 r + p_2 s)} \left[ e^{-i\bar{\varepsilon}_j(t_1 - t_0)} e^{i\bar{\varepsilon}_k^*(t_2 - t_0)} \left[ \Psi\left(\frac{1}{2} - \frac{\beta}{2\pi i}(\bar{\varepsilon}_j - \mu)\right) \right. \right. \\
& \left. \left. - \Psi\left(\frac{1}{2} - \frac{\beta}{2\pi i}(\bar{\varepsilon}_k^* - \mu - V_{\gamma} - \Omega_{\gamma}(p_1 r + p_2 s))\right) \right] + e^{-i\bar{\varepsilon}_j(t_1 - t_0)} e^{i(\mu + V_{\gamma} + \Omega_{\gamma}(p_1 r + p_2 s))(t_2 - t_0)} \right. \\
& \left. \left. \times [\bar{\Phi}(t_2 - t_0, \beta, -(\bar{\varepsilon}_j - \mu)) - \bar{\Phi}(t_2 - t_0, \beta, -(\bar{\varepsilon}_k^* - \mu - V_{\gamma} - \Omega_{\gamma}(p_1 r + p_2 s)))] \right] \right\}
\end{aligned}$$

$$\begin{aligned}
& + i \sum_{r,r',s,s'} J_r \left( \frac{A_\gamma^{(1)}}{p_1 \Omega_\gamma} \right) J_{r'} \left( \frac{A_\gamma^{(1)}}{p_1 \Omega_\gamma} \right) J_s \left( \frac{A_\gamma^{(2)}}{p_2 \Omega_\gamma} \right) J_{s'} \left( \frac{A_\gamma^{(2)}}{p_2 \Omega_\gamma} \right) \frac{e^{-i(r-r')\phi_\gamma}}{\bar{\epsilon}_j - \bar{\epsilon}_k^* - \Omega_\gamma(p_1(r-r') + p_2(s-s'))} \\
& \times \left[ e^{-i\bar{\epsilon}_j(t_1-t_0)} e^{i\bar{\epsilon}_k^*(t_2-t_0)} \left[ \Psi \left( \frac{1}{2} + \frac{\beta}{2\pi i} (\bar{\epsilon}_j - \mu - V_\gamma - \Omega_\gamma(p_1 r + p_2 s)) \right) \right. \right. \\
& \left. \left. - \Psi \left( \frac{1}{2} - \frac{\beta}{2\pi i} (\bar{\epsilon}_k^* - \mu - V_\gamma - \Omega_\gamma(p_1 r' + p_2 s')) \right) \right] \right. \\
& \left. + e^{i\bar{\epsilon}_k^*(t_2-t_0)} e^{-i(\mu+V_\gamma+\Omega_\gamma(p_1 r+p_2 s))(t_1-t_0)} \left[ \bar{\Phi}(t_1-t_0, \beta, \bar{\epsilon}_j - \mu - V_\gamma - \Omega_\gamma(p_1 r + p_2 s)) \right. \right. \\
& \left. \left. - \bar{\Phi}(t_1-t_0, \beta, \bar{\epsilon}_k^* - \mu - V_\gamma - \Omega_\gamma(p_1 r' + p_2 s')) \right] \right. \\
& \left. + e^{-i\bar{\epsilon}_j(t_1-t_0)} e^{i(\mu+V_\gamma+\Omega_\gamma(p_1 r'+p_2 s'))(t_2-t_0)} \left[ \bar{\Phi}(t_2-t_0, \beta, -(\bar{\epsilon}_j - \mu - V_\gamma - \Omega_\gamma(p_1 r + p_2 s))) \right. \right. \\
& \left. \left. - \bar{\Phi}(t_2-t_0, \beta, -(\bar{\epsilon}_k^* - \mu - V_\gamma - \Omega_\gamma(p_1 r' + p_2 s'))) \right] \right. \\
& \left. + \theta(t_1-t_2) \left[ e^{-i\Omega_\gamma(p_1 r+p_2 s)(t_1-t_0)} e^{i\Omega_\gamma(p_1 r'+p_2 s')(t_2-t_0)} e^{-i(\mu+V_\gamma)(t_1-t_2)} \right. \right. \\
& \left. \left. \times \left[ \bar{\Phi}(t_1-t_2, \beta, \bar{\epsilon}_k^* - \mu - V_\gamma - \Omega_\gamma(p_1 r' + p_2 s')) - \bar{\Phi}(t_1-t_2, \beta, \bar{\epsilon}_j - \mu - V_\gamma - \Omega_\gamma(p_1 r + p_2 s)) \right] \right. \right. \\
& \left. \left. + e^{-i\bar{\epsilon}_j(t_1-t_2)} e^{-i\Omega_\gamma(p_1(r-r')+p_2(s-s'))(t_2-t_0)} \left[ \Psi \left( \frac{1}{2} - \frac{\beta}{2\pi i} (\bar{\epsilon}_j - \mu - V_\gamma - \Omega_\gamma(p_1 r + p_2 s)) \right) \right. \right. \right. \\
& \left. \left. - \Psi \left( \frac{1}{2} + \frac{\beta}{2\pi i} (\bar{\epsilon}_j - \mu - V_\gamma - \Omega_\gamma(p_1 r + p_2 s)) \right) \right] \right] \right. \\
& \left. + \theta(t_2-t_1) \left[ e^{-i\Omega_\gamma(p_1 r+p_2 s)(t_1-t_0)} e^{i\Omega_\gamma(p_1 r'+p_2 s')(t_2-t_0)} e^{-i(\mu+V_\gamma)(t_1-t_2)} \right. \right. \\
& \left. \left. \times \left[ \bar{\Phi}(t_2-t_1, \beta, -(\bar{\epsilon}_k^* - \mu - V_\gamma - \Omega_\gamma(p_1 r' + p_2 s'))) - \bar{\Phi}(t_2-t_1, \beta, -(\bar{\epsilon}_j - \mu - V_\gamma - \Omega_\gamma(p_1 r + p_2 s))) \right] \right] \right. \\
& \left. + e^{i\bar{\epsilon}_k^*(t_2-t_1)} e^{-i\Omega_\gamma(p_1(r-r')+p_2(s-s'))(t_1-t_0)} \left[ \Psi \left( \frac{1}{2} - \frac{\beta}{2\pi i} (\bar{\epsilon}_k^* - \mu - V_\gamma - \Omega_\gamma(p_1 r' + p_2 s')) \right) \right. \right. \\
& \left. \left. - \Psi \left( \frac{1}{2} + \frac{\beta}{2\pi i} (\bar{\epsilon}_k^* - \mu - V_\gamma - \Omega_\gamma(p_1 r' + p_2 s')) \right) \right] \right] \right] \Bigg\} \quad (E1)
\end{aligned}$$

The formula for the current in lead  $\alpha$  can be similarly derived by inserting Eq. (66) into Eq. (22) of Ref. [89]; we defer its publication to a forthcoming paper on the quantum pump. To evaluate the two-time current correlation function in Eq. (29) for the biharmonic driving model, it is necessary to evaluate the integral appearing in the expression (D7) for  $\Lambda_\beta^+(t_2, t_1)$ . Expanding the integrand using Eq. (66), we obtain

$$\begin{aligned}
& \int_{t_0}^{t_1} d\tau e^{i\bar{\epsilon}_j^*(t_1-\tau)} e^{-i\mu(t_2-\tau)} e^{-i\psi_\beta(t_2,\tau)} \operatorname{cosech} \left( \frac{\pi}{\beta} (t_2 - \tau) \right) \Big|_{t_2 \neq \tau} \\
& = \frac{\beta}{\pi} e^{i\bar{\epsilon}_j^*(t_1-t_0)} e^{-i(\mu+V_\beta)(t_2-t_0)} e^{-i\frac{A_\beta^{(1)}}{p_1 \Omega_\beta} \sin(p_1 \Omega_\beta (t_2-t_0) + \phi_\beta)} e^{-i\frac{A_\beta^{(2)}}{p_2 \Omega_\beta} \sin(p_2 \Omega_\beta (t_2-t_0))} \sum_{r,s} J_r \left( \frac{A_\beta^{(1)}}{p_1 \Omega_\beta} \right) J_s \left( \frac{A_\beta^{(2)}}{p_2 \Omega_\beta} \right) e^{ir\phi_\beta} \\
& \times \left\{ \theta(t_1-t_2) e^{-i(\bar{\epsilon}_j^* - \mu - V_\beta - \Omega_\beta(p_1 r + p_2 s))(t_2-t_0)} \left[ \Psi \left( \frac{1}{2} - \frac{\beta}{2\pi i} (\bar{\epsilon}_j^* - \mu - V_\beta - \Omega_\beta(p_1 r + p_2 s)) \right) \right. \right. \\
& \left. \left. - \Psi \left( \frac{1}{2} + \frac{\beta}{2\pi i} (\bar{\epsilon}_j^* - \mu - V_\beta - \Omega_\beta(p_1 r + p_2 s)) \right) \right] - \bar{\Phi}(t_2-t_0, \beta, \bar{\epsilon}_j^* - \mu - V_\beta - \Omega_\beta(p_1 r + p_2 s)) \right. \\
& \left. + e^{-i(\bar{\epsilon}_j^* - \mu - V_\beta - \Omega_\beta(p_1 r + p_2 s))(t_1-t_0)} \left[ \theta(t_1-t_2) \bar{\Phi}(t_1-t_2, \beta, -(\bar{\epsilon}_j^* - \mu - V_\beta - \Omega_\beta(p_1 r + p_2 s))) \right. \right. \\
& \left. \left. + \theta(t_2-t_1) \bar{\Phi}(t_2-t_1, \beta, \bar{\epsilon}_j^* - \mu - V_\beta - \Omega_\beta(p_1 r + p_2 s)) \right] \right\}. \quad (E2)
\end{aligned}$$

The integral in  $(\Lambda_\beta^-)^\dagger(t_2, t_1)$  is obtained as the complex conjugate of Eq. (E2), the integral in  $\Lambda_\alpha^-(t_1, t_2)$  is obtained by exchanging indices  $\alpha \leftrightarrow \beta$  and times  $t_1 \leftrightarrow t_2$ , and the integral in  $(\Lambda_\alpha^+)^\dagger(t_1, t_2)$  is obtained as the complex conjugate of the latter expression.

Thus, one obtains for the  $\Lambda^\pm$  matrices

$$\begin{aligned} \Lambda_\beta^+(t_2, t_1) = & \sum_j \frac{\Gamma_\beta |\varphi_j^L \langle \varphi_j^R |}{\langle \varphi_j^R | \varphi_j^L \rangle} \left[ -\frac{i}{2\pi} e^{i\bar{\epsilon}_j^*(t_1-t_0)} e^{-i(\mu+V_\beta)(t_2-t_0)} e^{-i\frac{A_\beta^{(1)}}{p_1\Omega_\beta} \sin(p_1\Omega_\beta(t_2-t_0)+\phi_\beta)} e^{-i\frac{A_\beta^{(2)}}{p_2\Omega_\beta} \sin(p_2\Omega_\beta(t_2-t_0)} \right. \\ & \times \left[ e^{i\frac{A_\beta^{(1)}}{p_1\Omega_\beta} \sin(\phi_\beta)} \bar{\Phi}(\beta, t_2 - t_0, \bar{\epsilon}_j^* - \mu) + \sum_{r,s} J_r \left( \frac{A_\beta^{(1)}}{p_1\Omega_\beta} \right) J_s \left( \frac{A_\beta^{(2)}}{p_2\Omega_\beta} \right) e^{ir\phi_\beta} \left\{ \theta(t_1 - t_2) e^{-i(\bar{\epsilon}_j^* - \mu - V_\beta - \Omega_\beta(p_1r + p_2s))(t_2-t_0)} \right. \right. \\ & \times \left[ \Psi \left( \frac{1}{2} - \frac{\beta}{2\pi i} (\bar{\epsilon}_j^* - \mu - V_\beta - \Omega_\beta(p_1r + p_2s)) \right) - \Psi \left( \frac{1}{2} + \frac{\beta}{2\pi i} (\bar{\epsilon}_j^* - \mu - V_\beta - \Omega_\beta(p_1r + p_2s)) \right) \right] \\ & - \bar{\Phi}(t_2 - t_0, \beta, \bar{\epsilon}_j^* - \mu - V_\beta - \Omega_\beta(p_1r + p_2s)) \\ & + e^{-i(\bar{\epsilon}_j^* - \mu - V_\beta - \Omega_\beta(p_1r + p_2s))(t_1-t_0)} \left[ \theta(t_1 - t_2) \bar{\Phi}(t_1 - t_2, \beta, -(\bar{\epsilon}_j^* - \mu - V_\beta - \Omega_\beta(p_1r + p_2s))) \right. \\ & \left. \left. + \theta(t_2 - t_1) \bar{\Phi}(t_2 - t_1, \beta, \bar{\epsilon}_j^* - \mu - V_\beta - \Omega_\beta(p_1r + p_2s)) \right] \right] - \theta(t_1 - t_2) \frac{e^{i\bar{\epsilon}_j^*(t_1-t_2)}}{2} \Bigg], \end{aligned} \quad (\text{E3})$$

$$\begin{aligned} \Lambda_\alpha^-(t_1, t_2) = & \sum_j \frac{\Gamma_\alpha |\varphi_j^L \langle \varphi_j^R |}{\langle \varphi_j^R | \varphi_j^L \rangle} \left[ -\frac{i}{2\pi} e^{i\bar{\epsilon}_j^*(t_2-t_0)} e^{-i(\mu+V_\alpha)(t_1-t_0)} e^{-i\frac{A_\alpha^{(1)}}{p_1\Omega_\alpha} \sin(p_1\Omega_\alpha(t_1-t_0)+\phi_\alpha)} e^{-i\frac{A_\alpha^{(2)}}{p_2\Omega_\alpha} \sin(p_2\Omega_\alpha(t_1-t_0)} \right. \\ & \times \left[ e^{i\frac{A_\alpha^{(1)}}{p_1\Omega_\alpha} \sin(\phi_\alpha)} \bar{\Phi}(\beta, t_1 - t_0, \bar{\epsilon}_j^* - \mu) + \sum_{r,s} J_r \left( \frac{A_\alpha^{(1)}}{p_1\Omega_\alpha} \right) J_s \left( \frac{A_\alpha^{(2)}}{p_2\Omega_\alpha} \right) e^{ir\phi_\alpha} \left\{ \theta(t_2 - t_1) e^{-i(\bar{\epsilon}_j^* - \mu - V_\alpha - \Omega_\alpha(p_1r + p_2s))(t_1-t_0)} \right. \right. \\ & \times \left[ \Psi \left( \frac{1}{2} - \frac{\beta}{2\pi i} (\bar{\epsilon}_j^* - \mu - V_\alpha - \Omega_\alpha(p_1r + p_2s)) \right) - \Psi \left( \frac{1}{2} + \frac{\beta}{2\pi i} (\bar{\epsilon}_j^* - \mu - V_\alpha - \Omega_\alpha(p_1r + p_2s)) \right) \right] \\ & - \bar{\Phi}(t_1 - t_0, \beta, \bar{\epsilon}_j^* - \mu - V_\alpha - \Omega_\alpha(p_1r + p_2s)) \\ & + e^{-i(\bar{\epsilon}_j^* - \mu - V_\alpha - \Omega_\alpha(p_1r + p_2s))(t_2-t_0)} \left[ \theta(t_1 - t_2) \bar{\Phi}(t_1 - t_2, \beta, \bar{\epsilon}_j^* - \mu - V_\alpha - \Omega_\alpha(p_1r + p_2s)) \right. \\ & \left. \left. + \theta(t_2 - t_1) \bar{\Phi}(t_2 - t_1, \beta, -(\bar{\epsilon}_j^* - \mu - V_\alpha - \Omega_\alpha(p_1r + p_2s))) \right] \right] + \theta(t_2 - t_1) \frac{e^{i\bar{\epsilon}_j^*(t_2-t_1)}}{2} \Bigg]. \end{aligned} \quad (\text{E4})$$

The matrices  $(\Lambda_\beta^-)^\dagger(t_2, t_1)$  and  $(\Lambda_\alpha^+)^\dagger(t_1, t_2)$  are then obtained via complex conjugation and exchange of the lead indices  $\alpha \leftrightarrow \beta$  and times  $t_1 \leftrightarrow t_2$  in Eqs. (E3) and (E4), respectively.

- 
- [1] A. J. Bergren, L. Zeer-Wanklyn, M. Semple, N. Pekas, B. Szeto, and R. L. McCreery, Musical molecules: The molecular junction as an active component in audio distortion circuits, *J. Phys.: Condens. Matter* **28**, 094011 (2016).
- [2] J. M. Shalf and R. Leland, Computing beyond Moore's Law, *Computer* **48**, 14 (2015).
- [3] Y. Selzer and U. Peskin, Transient dynamics in molecular junctions: Picosecond resolution from dc measurements by a laser pulse pair sequence excitation, *J. Phys. Chem. C* **117**, 22369 (2013).
- [4] A. Aviram and M. A. Ratner, Molecular Rectifiers, *Chem. Phys. Lett.* **29**, 277 (1974).
- [5] A. S. Blum, J. C. Yang, R. Shashidhar, and B. Ratna, Comparing the conductivity of molecular wires with the scanning tunneling microscope, *Appl. Phys. Lett.* **82**, 3322 (2003).
- [6] C. H. Wohlgamuth, M. A. McWilliams, and J. D. Slinker, DNA as a molecular wire: Distance and sequence dependence, *Anal. Chem.* **85**, 8634 (2013).
- [7] L. P. Rokhinson, L. J. Guo, S. Y. Chou, and D. C. Tsui, Double-dot charge transport in Si single electron/hole transistors, *Appl. Phys. Lett.* **76**, 4 (2000).
- [8] T. M. Swager, The molecular wire approach to sensory signal amplification, *Acc. Chem. Res.* **31**, 201 (1998).
- [9] I. Iñiguez-de-la Torre, T. González, D. Pardo, C. Gardès, Y. Roelens, S. Bollaert, A. Curutchet, C. Gaquiere, and J. Mateos, Three-terminal junctions operating as mixers, frequency doublers and detectors: A broad-band frequency numerical and experimental study at room temperature, *Semicond. Sci. Technol.* **25**, 125013 (2010).
- [10] S. J. van der Molen and P. Liljeroth, Charge transport through molecular switches, *J. Phys.: Condens. Matter* **22**, 133001 (2010).
- [11] W. Liu, S. N. Filimonov, J. Carrasco, and A. Tkatchenko, Molecular switches from benzene derivatives adsorbed on metal surfaces, *Nat. Commun.* **4**, 2569 (2013).
- [12] H. Drexler, J. S. Scott, S. J. Allen, K. L. Campman, and A. C. Gossard, Photon-assisted tunneling in a resonant tun-



- neling diode: Stimulated emission and absorption in the THz range, *Appl. Phys. Lett.* **67**, 2816 (1995).
- [13] M. Covington, M. W. Keller, R. L. Kautz, and J. Martinis, Photon-Assisted Tunneling in Electron Pumps, *Phys. Rev. Lett.* **84**, 5192 (2000).
- [14] S. Li, Z. Yu, S.-F. Yen, W. C. Tang, and P. J. Burke, Carbon nanotube transistor operation at 2.6 GHz, *Nano Lett.* **4**, 753 (2004).
- [15] P. J. Burke, Carbon nanotube devices for GHz to THz applications, *Proc. SPIE* **5593**, 52 (2004).
- [16] J. Chaste, L. Lechner, P. Morfin, G. Feve, T. Kontos, J. M. Berroir, D. C. Glattli, H. Happy, P. Hakonen, and B. Placais, Single carbon nanotube transistor at GHz frequency, *Nano Lett.* **8**, 525 (2008).
- [17] W. Zhang, P. H. Q. Pham, E. R. Brown, and P. J. Burke, AC conductivity parameters of graphene derived from THz etalon transmittance, *Nanoscale* **6**, 13895 (2014).
- [18] M. Ratner, A brief history of molecular electronics, *Nat. Nanotechnol.* **8**, 378 (2013).
- [19] Y. M. Blanter and M. Büttiker, Shot noise in mesoscopic conductors, *Phys. Rep.* **336**, 1 (2000).
- [20] M. Reznikov, M. Heiblum, H. Shtrikman, and D. Mahalu, Temporal Correlation of Electrons: Suppression of Shot Noise in a Ballistic Quantum Point Contact, *Phys. Rev. Lett.* **75**, 3340 (1995).
- [21] A. Kumar, L. Saminadayar, D. Glattli, Y. Jin, and B. Etienne, Experimental Test of the Quantum Shot Noise Reduction Theory, *Phys. Rev. Lett.* **76**, 2778 (1996).
- [22] L. Saminadayar, D. Glattli, Y. Jin, and B. Etienne, Observation of the  $e/3$  Fractionally Charged Laughlin Quasiparticle, *Phys. Rev. Lett.* **79**, 2526 (1997).
- [23] D. Djukic and J. M. van Ruitenbeek, Shot noise measurements on a single molecule, *Nano Lett.* **6**, 789 (2006).
- [24] M. A. Ochoa, Y. Selzer, U. Peskin, and M. Galperin, Pump-probe noise spectroscopy of molecular junctions, *J. Phys. Chem. Lett.* **6**, 470 (2015).
- [25] F. D. Parmentier, L. N. Serkovic-Loli, P. Roulleau, and D. C. Glattli, Photon-Assisted Shot Noise in Graphene in the Terahertz Range, *Phys. Rev. Lett.* **116**, 227401 (2016).
- [26] H. Nyquist, Thermal agitation of electric charge in conductors, *Phys. Rev.* **32**, 110 (1928).
- [27] J. B. Johnson, Thermal agitation of electricity in conductors, *Phys. Rev.* **32**, 97 (1928).
- [28] R. Aguado and L. P. Kouwenhoven, Double Quantum Dots as Detectors of High-Frequency Quantum Noise in Mesoscopic Conductors, *Phys. Rev. Lett.* **84**, 1986 (2000).
- [29] U. Gavish, Y. Levinson, and Y. Imry, Detection of quantum noise, *Phys. Rev. B* **62**, R10637 (2000).
- [30] P. M. Billangeon, F. Pierre, H. Bouchiat, and R. Deblock, Emission and Absorption Asymmetry in the Quantum Noise of a Josephson Junction, *Phys. Rev. Lett.* **96**, 136804 (2006).
- [31] R. Zamoum, M. Lavagna, and A. Crépieux, Non-symmetrized noise in a quantum dot: Interpretation in terms of photon emission and coherent superposition of scattering paths, *Phys. Rev. B* **93**, 235449 (2016).
- [32] S. R. Eric Yang, Quantum shot noise spectrum of a point contact, *Solid State Commun.* **81**, 375 (1992).
- [33] M. Büttiker, Scattering theory of current and intensity noise correlations in conductors and wave guides, *Phys. Rev. B* **46**, 12485 (1992).
- [34] M. Büttiker, Role of scattering amplitudes in frequency-dependent current fluctuations in small conductors, *Phys. Rev. B* **45**, 3807 (1992).
- [35] B. H. Wu and C. Timm, Noise spectra of ac-driven quantum dots: Floquet master-equation approach, *Phys. Rev. B* **81**, 075309 (2010).
- [36] O. Entin-Wohlman, Y. Imry, S. A. Gurvitz, and A. Aharony, Steps and dips in the ac conductance and noise of mesoscopic structures, *Phys. Rev. B* **75**, 193308 (2007).
- [37] E. A. Rothstein, O. Entin-Wohlman, and A. Aharony, Noise spectra of a biased quantum dot, *Phys. Rev. B* **79**, 075307 (2009).
- [38] N. Gabdank, E. A. Rothstein, O. Entin-Wohlman, and A. Aharony, Noise spectra of an interacting quantum dot, *Phys. Rev. B* **84**, 235435 (2011).
- [39] M. Büttiker, Scattering Theory of Thermal and Excess Noise in Open Conductors, *Phys. Rev. Lett.* **65**, 2901 (1990).
- [40] R. Landauer, Solid-state shot noise, *Phys. Rev. B* **47**, 16427 (1993).
- [41] H. E. van den Brom and J. M. van Ruitenbeek, Quantum suppression of Shot Noise in Atom-Size Metallic Contacts, *Phys. Rev. Lett.* **82**, 1526 (1999).
- [42] L. Dicarolo, J. R. Williams, Y. Zhang, D. T. McClure, and C. M. Marcus, Shot Noise in Graphene, *Phys. Rev. Lett.* **100**, 156801 (2008).
- [43] R. Schoelkopf, P. Burke, A. Kozhevnikov, D. Prober, and M. Rooks, Frequency Dependence of Shot Noise in a Diffusive Mesoscopic Conductor, *Phys. Rev. Lett.* **78**, 3370 (1997).
- [44] J. Gabelli and B. Reulet, Dynamics of Quantum Noise in a Tunnel Junction Under ac Excitation, *Phys. Rev. Lett.* **100**, 026601 (2008).
- [45] M. Moskalets and M. Büttiker, Floquet scattering theory for current and heat noise in large amplitude adiabatic pumps, *Phys. Rev. B* **70**, 245305 (2004).
- [46] M. Moskalets and M. Büttiker, Time-resolved noise of adiabatic quantum pumps, *Phys. Rev. B* **75**, 035315 (2007).
- [47] M. Moskalets, *Scattering Matrix Approach to Non-Stationary Quantum Transport* (Imperial College Press, London, 2012).
- [48] J. H. Dai and R. Zhu, Fano resonance in the nonadiabatic pumped shot noise of a time-dependent quantum well, *Eur. Phys. J. B* **87**, 288 (2014).
- [49] R. Zhu, J. H. Dai, and Y. Guo, Fano resonance in the nonadiabatically pumped shot noise of a time-dependent quantum well in a two-dimensional electron gas and graphene, *J. Appl. Phys.* **117**, 164306 (2015).
- [50] S. Camalet, S. Kohler, and P. Hänggi, Shot-noise control in ac-driven nanoscale conductors, *Phys. Rev. B* **70**, 155326 (2004).
- [51] G. B. Lesovik and L. S. Levitov, Noise in an ac Biased Junction: Nonstationary Aharonov-Bohm Effect, *Phys. Rev. Lett.* **72**, 538 (1994).
- [52] J. Lehmann, S. Kohler, V. May, and P. Hänggi, Vibrational effects in laser-driven molecular wires, *J. Chem. Phys.* **121**, 2278 (2004).
- [53] M. Vanević and W. Belzig, Control of electron-hole pair generation by biharmonic voltage drive of a quantum point contact, *Phys. Rev. B* **86**, 241306 (2012).

- [54] V. S. Rychkov, M. L. Polianski, and M. Büttiker, Photon-assisted electron-hole shot noise in multiterminal conductors, *Phys. Rev. B* **72**, 155326 (2005).
- [55] M. Vanević, Y. V. Nazarov, and W. Belzig, Elementary charge-transfer processes in mesoscopic conductors, *Phys. Rev. B* **78**, 245308 (2008).
- [56] D. A. Ivanov, H. W. Lee, and L. S. Levitov, Coherent states of alternating current, *Phys. Rev. B* **56**, 6839 (1997).
- [57] J. Keeling, I. Klich, and L. S. Levitov, Minimal Excitation States of Electrons in One-Dimensional Wires, *Phys. Rev. Lett.* **97**, 116403 (2006).
- [58] J. Dubois, T. Jullien, F. Portier, P. Roche, A. Cavanna, Y. Jin, W. Wegscheider, P. Roulleau, and D. C. Glatli, Minimal-excitation states for electron quantum optics using levitons, *Nature (London)* **502**, 659 (2013).
- [59] J. Gabelli and B. Reulet, Shaping a time-dependent excitation to minimize the shot noise in a tunnel junction, *Phys. Rev. B* **87**, 075403 (2013).
- [60] M. H. Pedersen and M. Büttiker, Scattering theory of photon-assisted electron transport, *Phys. Rev. B* **58**, 12993 (1998).
- [61] J. Hammer and W. Belzig, Quantum noise in ac-driven resonant-tunneling double-barrier structures: Photon-assisted tunneling versus electron antibunching, *Phys. Rev. B* **84**, 085419 (2011).
- [62] M. Strass, P. Hänggi, and S. Kohler, Nonadiabatic Electron Pumping: Maximal Current with Minimal Noise, *Phys. Rev. Lett.* **95**, 130601 (2005).
- [63] R. P. Riwar, J. Splettstoesser, and J. König, Zero-frequency noise in adiabatically driven interacting quantum systems, *Phys. Rev. B* **87**, 195407 (2013).
- [64] C. G. Rocha, L. E. F. Foa Torres, and G. Cuniberti, ac transport in graphene-based Fabry-Pérot devices, *Phys. Rev. B* **81**, 115435 (2010).
- [65] O. V. Konstantinov and V. I. Perel', A diagram technique for evaluating transport quantities, *ZhETF* **39**, 197 (1961) [*Sov. Phys.-JETP* **12**, 142 (1961)].
- [66] L. P. Kadanoff and G. Baym, *Quantum Statistical Mechanics: Green's Function Methods in Equilibrium and Nonequilibrium Problems* (Benjamin, New York, 1962).
- [67] L. V. Keldysh, Diagram Technique for Nonequilibrium Processes, *ZhETF* **47**, 1515 (1965) [*Sov. Phys.-JETP* **20**, 1018 (1965)].
- [68] G. Stefanucci and R. van Leeuwen, *Nonequilibrium Many-Body Theory of Quantum Systems: A Modern Introduction* (Cambridge University Press, Cambridge, UK, 2013).
- [69] L. Arrachea and M. Moskalets, Relation between scattering-matrix and Keldysh formalisms for quantum transport driven by time-periodic fields, *Phys. Rev. B* **74**, 245322 (2006).
- [70] M. Di Ventra, *Electrical Transport in Nanoscale Systems* (Cambridge University Press, Cambridge, UK, 2008).
- [71] K. Joho, S. Maier, and A. Komnik, Transient noise spectra in resonant tunneling setups: Exactly solvable models, *Phys. Rev. B* **86**, 155304 (2012).
- [72] H. Ness and L. K. Dash, Nonequilibrium fluctuation-dissipation relations for one- and two-particle correlation functions in steady-state quantum transport, *J. Chem. Phys.* **140** (2014).
- [73] C. Caroli, R. Combescot, and P. Nozieres, Direct calculation of the tunneling current, *Science* **4**, 916 (1971).
- [74] C. Caroli, R. Combescot, D. Lederer, P. Nozieres, and D. Saint-James, A direct calculation of the tunneling current. II. Free electron description, *J. Phys. C: Solid State Phys.* **4**, 2598 (1971).
- [75] N. S. Wingreen, A. P. Jauho, and Y. Meir, Time-dependent transport through a mesoscopic structure, *Phys. Rev. B* **48**, 8487 (1993).
- [76] A. P. Jauho, N. S. Wingreen, and Y. Meir, Time-dependent transport in interacting and noninteracting resonant-tunneling systems, *Phys. Rev. B* **50**, 5528 (1994).
- [77] G. Stefanucci and C. O. Almbladh, Time-dependent partition-free approach in resonant tunneling systems, *Phys. Rev. B* **69**, 195318 (2004).
- [78] R. Tuovinen, N. Säkkinen, D. Karlsson, G. Stefanucci, and R. van Leeuwen, Phononic heat transport in the transient regime: An analytic solution, *Phys. Rev. B* **93**, 214301 (2016).
- [79] M. Cini, Time-dependent approach to electron transport through junctions: General theory and simple applications, *Phys. Rev. B* **22**, 5887 (1980).
- [80] P.-Y. Yang, C.-Y. Lin, and W.-M. Zhang, Master equation approach to transient quantum transport incorporating initial correlations, *Phys. Rev. B* **92**, 165403 (2015).
- [81] Z. Feng, J. Maciejko, J. Wang, and H. Guo, Current fluctuations in the transient regime: An exact formulation for mesoscopic systems, *Phys. Rev. B* **77**, 075302 (2008).
- [82] P.-Y. Yang, C.-Y. Lin, and W.-M. Zhang, Transient current-current correlations and noise spectra, *Phys. Rev. B* **89**, 115411 (2014).
- [83] E. Perfetto, G. Stefanucci, and M. Cini, Spin-flip scattering in time-dependent transport through a quantum dot: Enhanced spin-current and inverse tunneling magnetoresistance, *Phys. Rev. B* **78**, 155301 (2008).
- [84] R. Tuovinen, R. van Leeuwen, E. Perfetto, and G. Stefanucci, Time-dependent Landauer-Büttiker formula for transient dynamics, *J. Phys.: Conf. Ser.* **427**, 012014 (2013).
- [85] R. Tuovinen, E. Perfetto, G. Stefanucci, and R. van Leeuwen, Time-dependent Landauer-Büttiker formula: Application to transient dynamics in graphene nanoribbons, *Phys. Rev. B* **89**, 085131 (2014).
- [86] C. G. da Rocha, R. Tuovinen, R. van Leeuwen, and P. Koskinen, Curvature in graphene nanoribbons generates temporally and spatially focused electric currents, *Nanoscale* **7**, 8627 (2015).
- [87] R. Tuovinen, Time-dependent quantum transport in nanosystems: A nonequilibrium green's function approach. Ph.D. thesis, University of Jyväskylä, 2016.
- [88] M. Ridley, A. Mackinnon, and L. Kantorovich, Current through a multilead nanojunction in response to an arbitrary time-dependent bias, *Phys. Rev. B* **91**, 125433 (2015).
- [89] M. Ridley, A. MacKinnon, and L. Kantorovich, Calculation of the current response in a nanojunction for an arbitrary time-dependent bias: Application to the molecular wire, *J. Phys.: Conf. Ser.* **696**, 012017 (2016).
- [90] R. Tuovinen, R. van Leeuwen, E. Perfetto, and G. Stefanucci, Time-dependent Landauer-Büttiker formalism for superconducting junctions at arbitrary temperatures, *J. Phys.: Conf. Ser.* **696**, 012016 (2016).

- [91] M. Ridley, A. MacKinnon, and L. Kantorovich, Fluctuating-bias controlled electron transport in molecular junctions, *Phys. Rev. B* **93**, 205408 (2016).
- [92] B. Gaury and X. Waintal, Dynamical control of interference using voltage pulses in the quantum regime, *Nat. Commun.* **5**, 3844 (2014).
- [93] D. Langreth and J. Wilkins, Theory of Spin Resonance in Dilute Magnetic Alloys, *Phys. Rev. B* **6**, 3189 (1972).
- [94] D. C. Langreth, Linear and Nonlinear Response Theory with Applications, in *NATO Advanced Studies Series B*, edited by J. T. Devreese and E. van Doren (Plenum, New York, 1976), pp. 3–32.
- [95] H.-A. Engel and D. Loss, Asymmetric Quantum Shot noise in Quantum Dots, *Phys. Rev. Lett.* **93**, 136602 (2004).
- [96] C. J. O. Verzijl and J. M. Thijssen, DFT-based molecular transport implementation in ADF/BAND, *J. Phys. Chem. C* **116**, 24393 (2012).
- [97] C. J. O. Verzijl, J. S. Seldenthuis, and J. M. Thijssen, Applicability of the wide-band limit in DFT-based molecular transport calculations, *J. Chem. Phys.* **138**, 094102 (2013).
- [98] E. Zakka-Bajjani, J. Ségala, F. Portier, P. Roche, D. C. Glatli, A. Cavanna, and Y. Jin, Experimental Test of the High-Frequency Quantum Shot Noise Theory in a Quantum Point Contact, *Phys. Rev. Lett.* **99**, 236803 (2007).
- [99] V. Mujica, M. Kemp, and M. A. Ratner, Electron conduction in molecular wires. I. A scattering formalism, *J. Chem. Phys.* **101**, 6849 (1994).
- [100] V. Mujica, M. Kemp, and M. A. Ratner, Electron conduction in molecular tunneling microscopy wires. II. application, *J. Chem. Phys.* **101**, 6856 (1994).
- [101] J. Lehmann, S. Kohler, P. Hänggi, and A. Nitzan, Molecular Wires Acting as Coherent Quantum Ratchets, *Phys. Rev. Lett.* **88**, 228305 (2002).
- [102] S. Chen, H. Xie, Y. Zhang, X. Cui, and G. Chen, Quantum transport through an array of quantum dots, *Nanoscale* **5**, 169 (2013).
- [103] M. Büttiker and R. Landauer, Traversal Time for Tunneling, *Phys. Rev. Lett.* **49**, 1739 (1982).
- [104] S. Collins, S. Lowe, and J. R. Barker, The quantum mechanical tunneling time problem-revisited, *J. Phys. C: Solid State Phys.* **20**, 6213 (1987).
- [105] T. Ozaki, Continued fraction representation of the Fermi-Dirac function for large-scale electronic structure calculations, *Phys. Rev. B* **75**, 035123 (2007).
- [106] A. Croy and U. Saalman, Propagation scheme for non-equilibrium dynamics of electron transport in nanoscale devices, *Phys. Rev. B* **80**, 245311 (2009).
- [107] J. Hu, R.-X. Xu, and Y. Yan, Communication: Padé spectrum decomposition of Fermi function and Bose function, *J. Chem. Phys.* **133**, 101106 (2010).
- [108] J. Hu, M. Luo, F. Jiang, R. X. Xu, and Y. Yan, Padéspectrum decompositions of quantum distribution functions and optimal hierarchical equations of motion construction for quantum open systems, *J. Chem. Phys.* **134**, 244106 (2011).
- [109] M. Lerch, Note sur la fonction, *Acta Math.* **11**, 19 (1887).